iScience

CellPress
OPEN ACCESS

Article

Sirtuin 1/sirtuin 3 are robust lysine delactylases and sirtuin 1-mediated delactylation regulates glycolysis

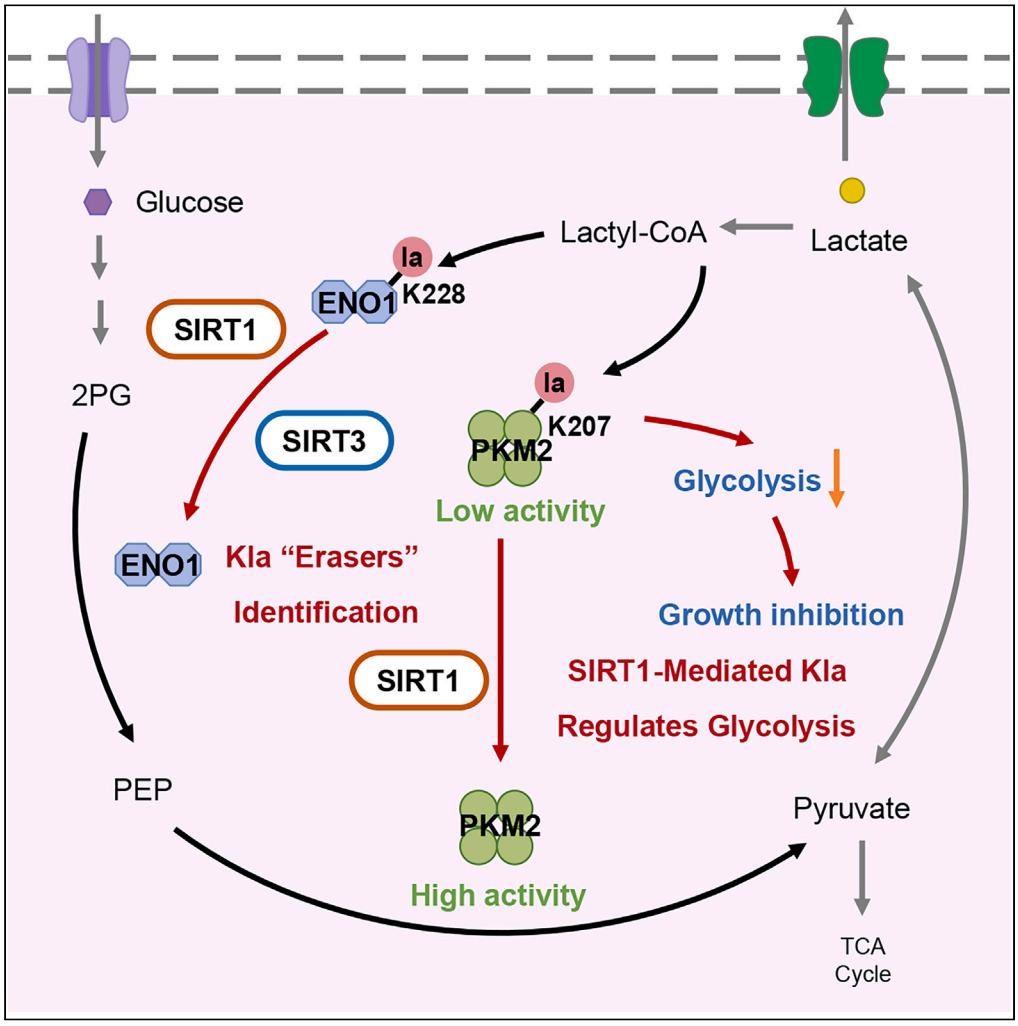

Runhua Du, Yanmei Gao, Cong Yan, ..., Mingyue Zheng, Jia Li, He Huang

hhuang@simm.ac.cn

Highlights

SIRT1 and SIRT3 as robust "erasers" of both histone and non-histone Kla

SIRT1 and SIRT3 show distinct regulatory patterns toward Kla

ENO1-K228la is a target of SIRT1/SIRT3, and PKM2-K207la is uniquely regulated by SIRT1

PKM2-K207la restricts glycolysis and cell proliferation by impeding PKM2 function

Du et al., iScience 27, 110911
October 18, 2024
https://doi.org/10.1016/j.isci.2024.110911

iScience

CellPress
OPEN ACCESS

Article

Sirtuin 1/sirtuin 3 are robust lysine delactylases and sirtuin 1-mediated delactylation regulates glycolysis

Runhua Du,[1,2] Yanmei Gao,[3] Cong Yan,[2] Xuelian Ren,[1,2] Shankang Qi,[2] Guobin Liu,[2] Xinlong Guo,[2] Xiaohan Song,[2] Hanmin Wang,[2] Jingxin Rao,[4] Yi Zang,[5] Mingyue Zheng,[4] Jia Li,[2] and He Huang[1,2,3,6,*]

SUMMARY

Lysine lactylation (Kla), an epigenetic mark triggered by lactate during glycolysis, including the Warburg effect, bridges metabolism and gene regulation. Enzymes such as p300 and HDAC1/3 have been pivotal in deciphering the regulatory dynamics of Kla, though questions about additional regulatory enzymes, their specific Kla substrates, and the underlying functional mechanisms persist. Here, we identify SIRT1 and SIRT3 as key "erasers" of Kla, shedding light on their selective regulation of both histone and non-histone proteins. Proteomic analysis in SIRT1/SIRT3 knockout HepG2 cells reveals distinct substrate specificities toward Kla, highlighting their unique roles in cellular signaling. Notably, we highlight the role of specific Kla modifications, such as those on the M2 splice isoform of pyruvate kinase (PKM2), in modulating metabolic pathways and cell proliferation, thereby expanding Kla's recognized functions beyond epigenetics. Therefore, this study deepens our understanding of Kla's functional mechanisms and broadens its biological significance.

INTRODUCTION

Protein post-translational modifications (PTMs) play essential roles in various physiological and pathological processes, contributing to almost all biological pathways.[1] Recent research has established connections between metabolite pools and PTMs, as many metabolites are substrates for enzymes involved in PTM pathways.[2] For example, acetyl-coenzyme A (CoA) can be used for lysine acetylation (Kac) by acetyltransferase through the mitochondrial oxidation of carbon sources such as glucose, amino acids, and fatty acids, or through the recycling of acetate groups. Similarly, S-adenosylmethionine (SAM), derived directly from the combined activities of serine-glycine-one carbon metabolism and the methionine cycle, can be employed by methyltransferases for lysine methylation.[2,3] These observations suggest that fluctuations in metabolite levels might affect the deposition and removal of chromatin modifications.

Lactate, a metabolite produced during glycolysis, is found at higher levels in cancer cells compared to normal cells, playing a crucial role in tumor occurrence and development.[4] Recently, a new type of epigenetic modification, histone lysine lactylation (Kla), derived from lactate, has been identified by us, providing insight into the mechanism linking lactate metabolism to metabolic rewiring and epigenetic remodeling.[5] Subsequent studies have also uncovered Kla on non-histone proteins and explored the roles of Kla under physiological and pathological conditions, such as in cancer, inflammation, stem cell regulation, embryonic development, neuropsychiatric disorders, homologous recombination repair and so on.[6–10]

Identifying key regulatory elements of the PTMs, such as the "writers," "erasers," and substrates, is essential for understanding their functions. In our initial study of Kla, we identified p300 as a promising histone Kla transferase.[5] Subsequently, HDAC1/3 and SIRT2 were found capable of removing Kla.[11–13] Recently, SIRT3 is reported to be an eraser of histone lactylation.[14] Despite these advancements, questions remain regarding whether other enzymes regulate Kla status and what specific Kla substrates are regulated by each enzyme, along with their functional preferences and switching mechanisms.

Sirtuins, a highly conserved family of nicotinamide adenine dinucleotide (NAD^+)-dependent deacylases, exhibit diverse actions, substrate affinities, and subcellular compartmentation.[15] Given the similarity of catalytic activity among sirtuins, in addition to SIRT2 and SIRT3, other sirtuin members may also serve as "erasers" for Kla, exerting differential regulation on it.

[1]School of Pharmaceutical Science and Technology, Hangzhou Institute for Advanced Study, University of Chinese Academy of Sciences, Hangzhou 310024, China
[2]State Key Laboratory of Chemical Biology, Shanghai Institute of Materia Medica, Chinese Academy of Sciences, Shanghai 201203, China
[3]School of Chinese Materia Medica, Nanjing University of Chinese Medicine, Nanjing 210023, China
[4]State Key Laboratory of Drug Discovery, Shanghai Institute of Materia Medica, Chinese Academy of Sciences, Shanghai 201203, China
[5]Lingang Laboratory, Shanghai 201203, China
[6]Lead contact
*Correspondence: hhuang@simm.ac.cn
https://doi.org/10.1016/j.isci.2024.110911

Here, our study reveals that SIRT1 and SIRT3 act as robust "erasers" of Kla both *in vitro* and in mammalian cells, affecting both histone and non-histone substrates. We quantitatively analyzed the Kla and Kac proteomes in wildtype (WT), SIRT1 knockout (KO), and SIRT3 KO HepG2 cells, successfully identifying 8075 Kla sites and 3515 Kac sites, respectively. Furthermore, we investigated the Kla and Kac substrates specifically regulated by SIRT1 or SIRT3. In total, 1348 Kla sites and 705 Kac sites were specifically mediated by SIRT1, while 1143 Kla sites and 177 Kac sites were specifically mediated by SIRT3. Notably, there was minimal overlap between the Kla and Kac substrates targeted by SIRT1 and SIRT3, suggesting distinct regulatory patterns of these two enzymes toward the two acylations. Pathway analysis revealed that while some of the Kla substrates regulated by SIRT1 and SIRT3 were enriched in similar pathways, such as spliceosome pathway, the pathways modulated by the Kla substrates targeted by these two delactylases also exhibited distinct preferences. For instance, SIRT1-targeted Kla proteins were significantly associated with RNA metabolism pathways, while Kla proteins regulated by SIRT3 tended to participate in inflammation and alcoholism-related pathways. However, SIRT3-targeted Kac proteins showed a preference for involvement in carbon metabolism. Importantly, we found that K228la of alpha-enolase (ENO1) is a target of SIRT1 and SIRT3, while K207la of PKM2 is specifically delactylased by SIRT1. We further demonstrated that PKM2-K207la reduces PKM2 activity by impeding tetramer formation and alters intracellular localization, subsequently inhibiting glycolysis and cell growth.

In summary, our study identifies SIRT1 and SIRT3 as robust "erasers" of the Kla pathway in mammalian cells and characterizes the SIRT1/SIRT3-regulated Kla and Kac substrate profiles. Bioinformatics analysis highlights the unique biological functions of SIRT1/SIRT3-targeted Kla and Kac proteins. Further functional studies elucidate the regulatory mechanisms of specific Kla sites on non-histone proteins, providing insights into the roles of Kla beyond epigenetics. These findings establish the essential foundation for further investigating the functional phenotype and mechanisms of Kla in depth.

RESULTS

Sirtuin 1 and sirtuin 3 extensively regulate lysine lactylation levels in mammalian cells

Our previous study has indicated that p300 functions as a "writer" for histone Kla,[5] followed by reports identifying HDAC1-3 and SIRT2 as "erasers" of histone Kla.[11,12] However, whether there are other "erasers" responsible for bulk delactylation, including both histones and non-histones, remain poorly understood. Given that sirtuins are a class of enzyme with NAD^+-dependent protein lysine deacylase activities,[16] we hypothesized that other sirtuins may also exhibit delactylation activity. Therefore, we carried out an *in vitro* assay using 7 recombinant sirtuins (including SIRT1-7) and core histones derived from HEK293T cells (Figure 1A). Our results showed that SIRT1-3 exhibited significant de-Kla activity toward core histones *in vitro*. To further confirm this result, we individually overexpressed SIRT1-3 in HEK293T cells. Consistent with the *in vitro* assay, overexpression of SIRT1 and SIRT3 markedly reduced the global level of Kla, while overexpression of SIRT2 had a minor effect on the global level of Kla (Figure 1B). These results preliminarily suggested that SIRT1 and SIRT3 can remove Kla both *in vitro* and *in vivo*. To further validate the Kla deacylase ability of SIRT1 and SIRT3, we constructed SIRT1 KO and SIRT3 KO cell lines in HepG2 cells. Western blot analysis comparing the levels of Kla and Kac in WT, SIRT1 KO, and SIRT3 KO HepG2 cells showed a significant increase in Kla level in both histone and non-histone proteins in SIRT1 KO and SIRT3 KO HepG2 cells, while Kac levels were slightly affected (Figures 1C, S1A, and S1B). Taken together, these results indicate that SIRT1 and SIRT3 are robust "erasers" of Kla, extensively regulating Kla levels in mammalian cells.

Proteome-wide identification of lysine lactylation and lysine acetylation substrates regulated by sirtuin 1 or sirtuin 3 in hepatocellular carcinomas cells

To gain insight into the landscape of SIRT1/SIRT3-targeted Kla substrates and the different regulatory mechanisms of SIRT1 and SIRT3 on Kla and Kac in HepG2 cells, we quantitatively analyzed the Kla and Kac proteomes in WT, SIRT1 KO, and SIRT3 KO HepG2 cells using HPLC-MS/MS (Figure 2A). Proteins extracted from WT, SIRT1 KO, and SIRT3 KO HepG2 cells were digested into peptides with trypsin. Subsequently, the peptides enriched by immunoprecipitation were subjected to HPLC-MS/MS analysis. Through this procedure, we successfully identified 8075 Kla sites on 2422 proteins and 3515 Kac sites on 1680 proteins (Tables S1 and S2). This result significantly expanded the map of Kla substrates, encompassing numerous non-histone substrates in addition to histones, indicating the widespread distribution of Kla proteins in mammalian cells.

Furthermore, we investigated the Kla and Kac substrates specifically regulated by SIRT1 or SIRT3 using a label-free quantitative method. The abundance of modified peptides was normalized to corresponding protein abundance to eliminate the influence of protein expression on modification abundance. Quantitative proteomics analysis showed that in HepG2 cells lacking SIRT1, 1348 Kla sites on 724 proteins were significantly upregulated (p-value <0.05 by t-test, Table S3), while 705 Kac sites on 477 proteins showed a similar increase (p-value <0.05 by t-test, Table S4) (Figure 2B). In SIRT3 KO HepG2 cells, 1143 Kla sites on 680 proteins exhibited a significant increase (p-value <0.05 by t-test, Table S5), while 177 Kac sites on 153 proteins displayed a similar increase (p-value <0.05 by t-test, Table S6) (Figure 2B). These results revealed the SIRT1/SIRT3-regulated Kla and Kac substrate profiles, indicating significant alterations in protein Kla levels in the absence of SIRT1 or SIRT3 and in mammalian cells.

Among the SIRT1/SIRT3-targeted Kla and Kac substrates, 450 SIRT1-targeted and 453 SIRT3-targeted proteins had a single Kla site, and 362 SIRT1-targeted and 133 SIRT3-targeted proteins had a single Kac site, while 41 and 18 proteins regulated by SIRT1 and SIRT3 respectively harbored at least 5 Kla sites, and only 11 proteins regulated by SIRT1 had more than 5 Kac sites (Figure 2C). Additionally, some proteins exhibited highly modified Kla in the absence of SIRT1 or SIRT3 (Figure 2D). For example, the neuroblast differentiation-associated protein AHNAK was the most lactylated protein, with 45 and 66 Kla sites upregulated by SIRT1 and SIRT3, respectively. Moreover, antigen KI-67 contained 30 Kla sites targeted by SIRT1 and 14 Kla sites targeted by SIRT3, making it the second most lactylated protein. However, the numbers

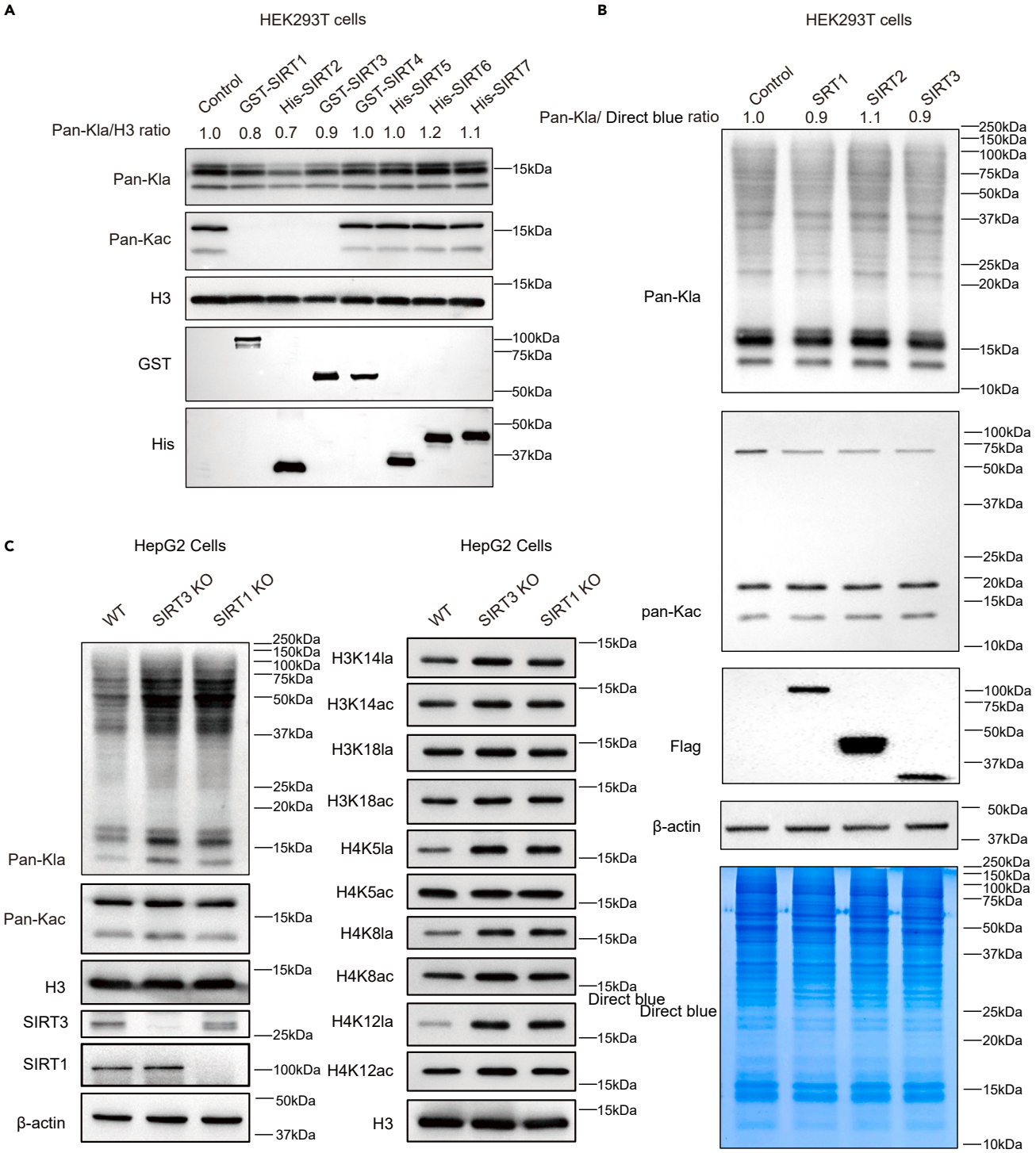

Figure 1. *In vitro* and *in vivo* screening of Kla deacylases

(A) *In vitro* screening of sirtuins' delactylase activities.

(B) Western blot analysis of Kla levels upon SIRT1-3 overexpression in HEK293T cells.

(C) Western blot analysis demonstrating increased Kla levels on both histones and non-histones upon knockout of SIRT1 and SIRT3 in HepG2 cells.

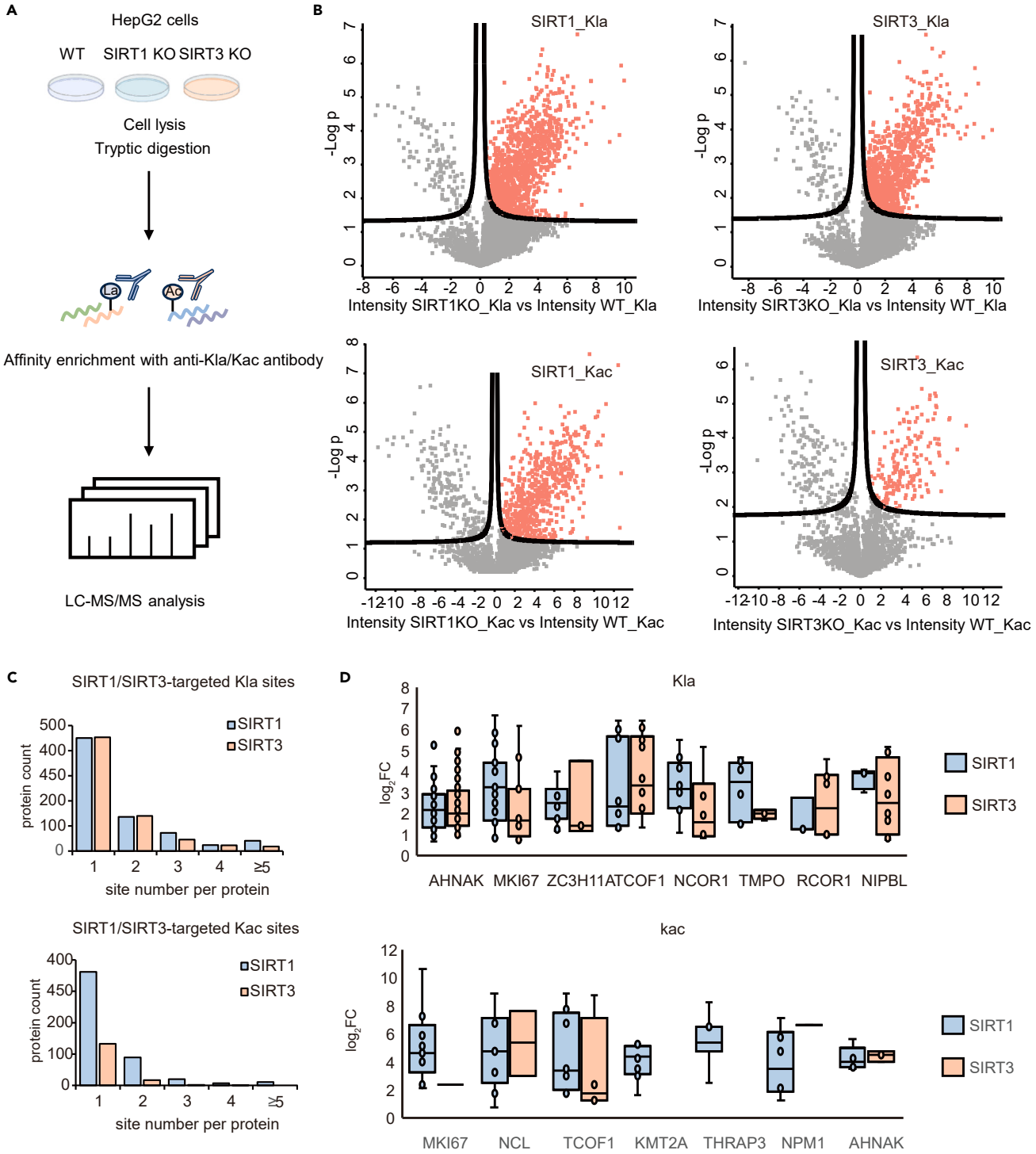

Figure 2. Identification of the global lysine lactylome and acetylome in HepG2 cells by HPLC-MS/MS

(A) Schematic overview of the experimental workflow for the identification of Kla and Kac in WT, SIRT1 KO, and SIRT3 KO HepG2 cells.

(B) Volcano plots representing the differentially expressed Kla and Kac sites between SIRT1 KO or SIRT3 KO versus WT HepG2 cells.

(C) Distribution of the number of SIRT1/SIRT3-targeted Kla and Kac sites identified per protein.

(D) The bar graph shows the fold change of lactylated and acetylated peptide intensities on the proteins highly regulated by SIRT1/SIRT3.

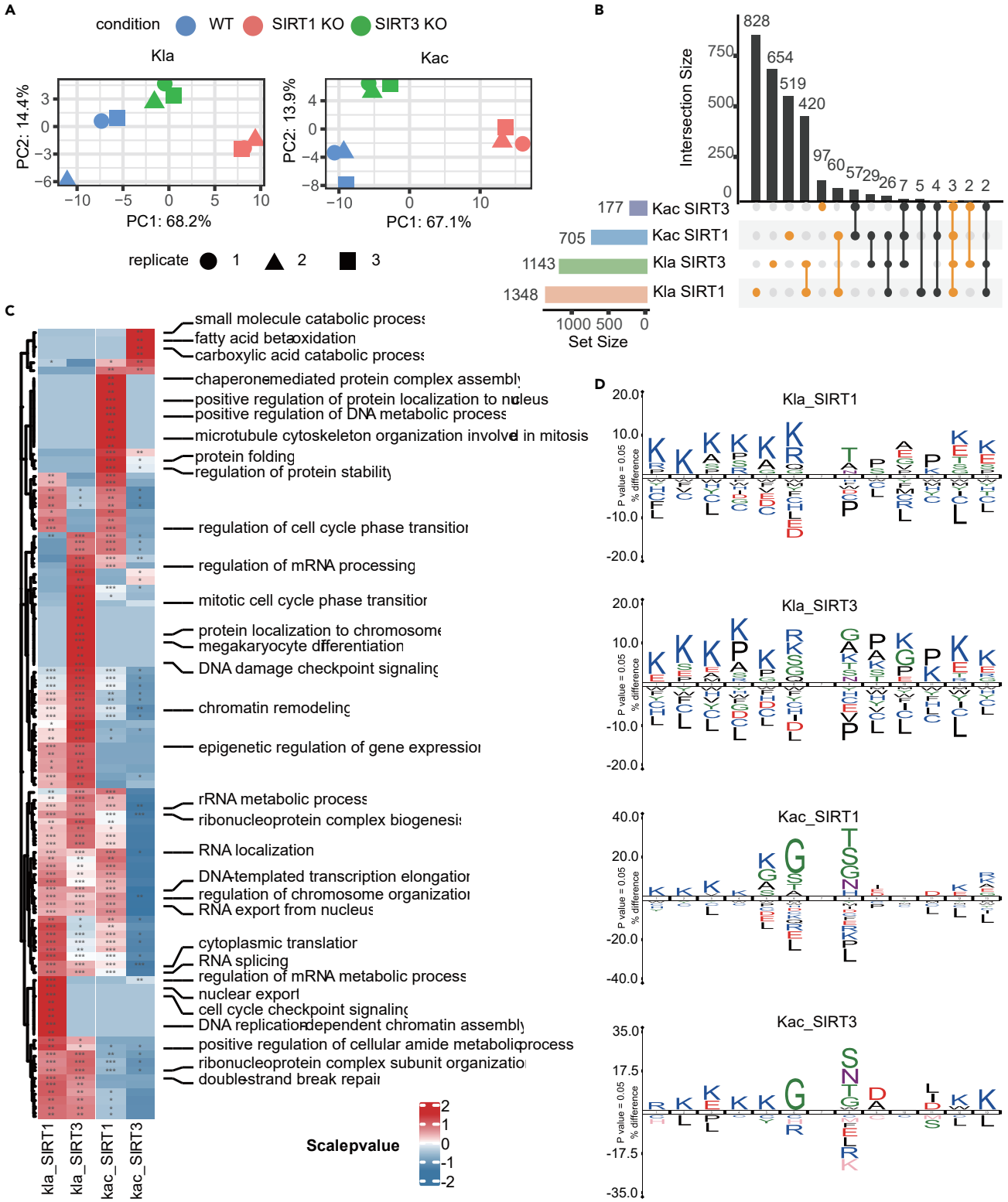
A
condition WT SIRT1 KO SIRT3 KO
Kla
Kac
PC2: 14.4%
PC1: 68.2%
PC2: 13.9%
PC1: 67.1%
replicate 1 2 3
B
Intersection Size
828
654
519
420
97
60
57
29
26
7
5
4
3
2
2
177 Kac SIRT3
705 Kac SIRT1
1143 Kla SIRT3
1348 Kla SIRT1
1000 500 0
Set Size
C
small molecule catabolic process
fatty acid beta-oxidation
carboxylic acid catabolic process
chaperone-mediated protein complex assembly
positive regulation of protein localization to nucleus
positive regulation of DNA metabolic process
microtubule cytoskeleton organization involved in mitosis
protein folding
regulation of protein stability
regulation of cell cycle phase transition
regulation of mRNA processing
mitotic cell cycle phase transition
protein localization to chromosome
megakaryocyte differentiation
DNA damage checkpoint signaling
chromatin remodeling
epigenetic regulation of gene expression
rRNA metabolic process
ribonucleoprotein complex biogenesis
RNA localization
DNA-templated transcription elongation
regulation of chromosome organization
RNA export from nucleus
cytoplasmic translation
RNA splicing
regulation of mRNA metabolic process
nuclear export
cell cycle checkpoint signaling
DNA replication-dependent chromatin assembly
positive regulation of cellular amide metabolic process
ribonucleoprotein complex subunit organization
double-strand break repair
kla_SIRT1
kla_SIRT3
kac_SIRT1
kac_SIRT3
Scale pvalue
2
1
0
-1
-2
D
Kla_SIRT1
Kla_SIRT3
Kac_SIRT1
Kac_SIRT3
P value = 0.05
% difference

Figure 3. Differential analysis of the global lysine lactylome and acetylome in SIRT1 KO and SIRT3 KO HepG2 cells

(A) PCA analysis of SIRT1/SIRT3-targeted Kla and Kac sites in WT, SIRT1 KO, and SIRT3 KO HepG2 cells.

(B) Distribution and comparison of the number of SIRT1/SIRT3-targeted Kla and Kac sites. The horizontal coordinates represent the total number of Kla and Kac sites that are specifically regulated by SIRT1/SIRT3, while the vertical coordinates represent the number of intersections between SIRT1/SIRT3-regulated Kla and Kac sites. Groups with intersections are connected by dots.

(C) Heatmap showing the degree of significant difference and GO enrichment pathway analysis of SIRT1 and SIRT3-targeted Kla and Kac sites. The hypergeometric distribution was applied to assess the enrichment of genes in specific pathways. *: $p < 0.05$, **: $p < 0.01$, ***: $p < 0.001$.

(D) Sequence motif logo showing a representative sequence for all Kla sites and Kac sites regulated by SIRT1 or SIRT3.

of Kac sites regulated by SIRT1/SIRT3 on AHNAK and antigen KI-67 were fewer than the Kla sites. The widespread occurrence of Kla substrates compared to Kac substrates underscores the significant role of SIRT1/SIRT3 in regulating Kla.

Sirtuin 1 and sirtuin 3 differentially regulate lysine lactylation and lysine acetylation

SIRT1 and SIRT3, both NAD^+-dependent deacylases within the sirtuins family,[17] exhibit highly divergent biological functions despite their relative conservation. This divergence arises from differences in enzymatic activities, unique binding partners and substrates, as well as distinct subcellular localization and expression patterns.[18] SIRT1, predominantly nuclear,[19] focuses on gene regulation, DNA repair, and metabolic control, influencing lifespan and stress resistance. Conversely, SIRT3 operates mainly in the mitochondria,[20] tuning metabolic pathways, antioxidant defenses, and fatty acid oxidation, crucial for energy metabolism and cellular responses to oxidative stress.[21,22] Their specialized roles reflect the diverse adaptions of sirtuins to manage cellular processes in different organelles. However, several reports have explicitly shown their overlapping roles in several physiological conditions. For example, both sirtuins contribute to the regulation of cellular metabolism, with SIRT1 influencing glucose and lipid metabolism in the nucleus and cytoplasm, and SIRT3 modulating mitochondrial metabolic pathways.[23,24] They also play roles in enhancing cellular resistance to stress and damage, with SIRT1 participating in DNA repair[25] and SIRT3 contributing to antioxidant defenses.[20] Additionally, both enzymes have been implicated in aging and longevity,[26,27] reflecting their shared importance in maintaining cellular health and homeostasis. Thus, to elucidate the roles of SIRT1 and SIRT3 in Kla and Kac pathways, we performed a differential analysis of Kla and Kac substrates regulated by these two enzymes.

Initially, we performed principal component analysis (PCA) to gain an overall perspective of the lysine lactylome and acetylome in the absence of SIRT1 or SIRT3. As expected, significant variations in Kla or Kac sites were observed in WT, SIRT1 KO, and SIRT3 KO HepG2 cells, indicating that the knockout of SIRT1 or SIRT3 stably and differentially affected distinct Kla and Kac substrate sites, thereby enabling unique biological functions (Figure 3A). Furthermore, we compared the overlap of SIRT1/SIRT3-targeted Kla/Kac sites and found a minimal overlap rate (Figure 3B). For instance, nearly 61.4% (828) of Kla sites targeted by SIRT1 (out of 1348 in total) were distinct from other SIRT3-targeted Kla sites or SIRT1/SIRT3-regulated Kac sites. Similarly, approximately 57.2% (654) of Kla sites targeted by SIRT3 (out of 1143 in total) were excluded from other Kla sites regulated by SIRT1 or SIRT1/SIRT3-targeted Kac sites (Figure 3B). Additionally, only 3 substrate sites overlapped, being both lactylated and acetylated, and regulated by both SIRT1 and SIRT3 (Figure 3B). Moreover, the negative correlation between SIRT1 and SIRT3 target Kla or Kac proteins further confirmed their differential regulation of Kla and Kac (Figures S2A and S2B).

To further explore the different biological functions of SIRT1 and SIRT3 targeted Kla and Kac proteins, we performed KEGG pathway analysis (Figure S2C). While SIRT1-targeted Kla and Kac sites, as well as SIRT3-targetd Kla sites, were most significantly enriched in the spliceosome pathway (adjusted p values are 3.28×10^{-26}, 3.07×10^{-23}, and 1.82×10^{-27}, respectively), indicating their participation in the same biological process, they also exhibited unique biological functions. Previous studies have shown that SIRT1 functions as a negative regulator of eukaryotic poly(A) RNA transport and plays a potentially important role in the RNA splicing pathway,[25,28] whereas SIRT3 serves as a crucial metabolic sensor regulating ATP generation, mitochondrial adaptive response to stress, and inflammation in wound macrophages post-injury.[29,30] KEGG pathway analysis showed that SIRT1-targeted Kla proteins were significantly enriched in the RNA transport pathway (adjusted $p = 6.55 \times 10^{-12}$), suggesting a relationship between Kla proteins and RNA metabolism, while Kla protein in SIRT3 KO cells tended to enrich in systemic lupus erythematosus (adjusted $p = 1.08 \times 10^{-14}$), neutrophil extracellular trap formation (adjusted $p = 1.47 \times 10^{-13}$), and alcoholism (adjusted $p = 1.81 \times 10^{-14}$). Interestingly, SIRT3-targeted Kac proteins were enriched in carbon metabolism (adjusted $p = 1.09 \times 10^{-7}$).

Given the distinct cellular localizations of SIRT1 and SIRT3, we also analyzed the SIRT1 and SIRT3 targeted substrates to determine the localization of modified proteins. The global lysine lactylome and acetylome (Figures S3A and S3B) demonstrated a significant nuclear prevalence for lactylation and acetylation sites, with 53.7% and 50.8% respectively. Furthermore, a notable proportion of these modifications (31% for lactylation and 28.9% for acetylation) were detected in the cytoplasm. In contrast, only a minor proportion of lactylation (2.3%) and acetylation (7.2%) sites were identified within the mitochondria. As previously reported, SIRT1 is primarily localized in the nucleus,[19] involved in the regulation of gene expression, DNA repair, and cell cycle.[25] It is, however, important to note that the localization of SIRT1 is not limited to the nuclear compartment. In defined physiological or pathological circumstances, SIRT1 exhibits a cytoplasmic presence,[31] actively contributing to vital cellular functions including metabolism, apoptosis, and autophagy.[15,32] Further analysis (Figures S3C and S3D) has revealed that 59.5% of the lactylation sites and 60.5% of the acetylation sites targeted by SIRT1 were located within the nucleus, while 30% of lactylation and 26.5% of acetylation sites were found in the cytoplasm. These findings indicated that proteins undergoing lactylation and acetylation regulated by SIRT1 predominantly reside in the nucleus and cytoplasm, which aligns with existing reports. Furthermore, SIRT3 is predominantly localized in the mitochondria.[33] However, emerging evidence suggests that under certain conditions, SIRT3 can exert functions within the nucleus, including DNA damage repair and transcriptional regulation.[34,35] For example, SIRT3 promotes non-homologous end-joining

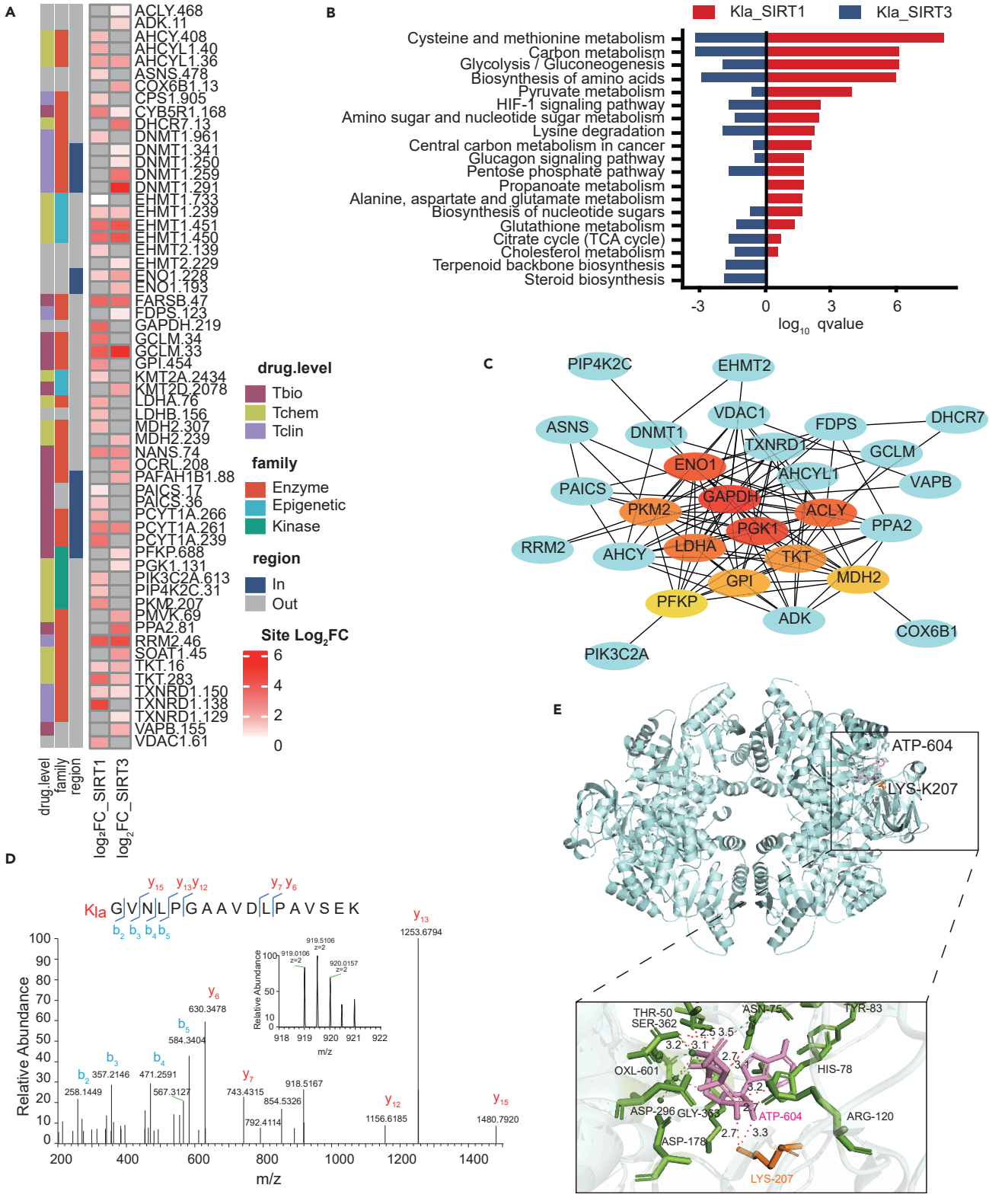

Figure 4. Function analysis of SIRT1 and SIRT3 targeted Kla sites associated with metabolism

(A) Heatmap showing the fold change of SIRT1 and SIRT3 targeted Kla sites associated with metabolism.

(B) KEGG pathway analysis depicting pathways enriched with SIRT1 and SIRT3 targeted Kla sites associated with metabolism.

Figure 4. *Continued*

(C) Interaction network of the SIRT1 and SIRT3-regulated Kla proteome based on the STRING database (v12.0). The network is visualized in Cytoscape (v3.8.2) using the cytoHubb plugin.

(D) Full MS and MS/MS spectra of PKM2 K207la peptide for its identification.

(E) Three-dimensional structure of PKM2 (PDB entry 4fxf) highlighting the important residues in the substrate binding pocked.

(NHEJ)-dependent DNA damage repair via the deacetylation of H3K56ac.[36] In addition, SIRT3 is reported to interact with nuclear envelope proteins and heterochromatin-associated proteins.[35] A subcellular localization analysis of the lactylation and acetylation sites regulated by SIRT3 (Figures S3E and S3F) indicated that 1.4% and 59.4% of the lactylation sites were distributed in the mitochondria and nucleus, respectively. In contrast, 17.6% of the acetylation sites regulated by SIRT3 were found in the mitochondria, whereas 40.5% were localized in the nucleus. The findings indicate that acetylation sites regulated by SIRT3 exhibit a greater tendency toward mitochondrial localization compared to lactylation sites, which display a higher propensity for nuclear localization. This implies that SIRT3 plays a role in distinct subcellular functions depending on the type of post-translational modification.

To enable a more precise comparison of regulatory variations between SIRT1 and SIRT3, as well as Kla and Kac, we performed Gene Ontology (GO) enrichment analysis via heatmaps and subsequently clustered the collected data (Figure 3C). Our results revealed distinct enrichment patterns, with SIRT1-targeted Kla sites preferentially involved in processes such as nuclear export (adjusted $p = 1.84 \times 10^{-12}$), DNA replication-dependent chromatin assembly (adjusted $p = 2.29 \times 10^{-10}$), and cell cycle checkpoint signaling (adjusted $p = 3.16 \times 10^{-7}$), while SIRT3-targeted Kla sites tended to be enriched in protein localization to chromosome (adjusted $p = 8.46 \times 10^{-17}$), megakaryocyte differentiation (adjusted $p = 6.98 \times 10^{-10}$), and DNA damage checkpoint signaling (adjusted $p = 4.59 \times 10^{-7}$). Mammalian SIRT3 is primarily located in the mitochondria.[20] However, it is also found in the nucleus where it deacetylates[37] and delactylases[14] histones. SIRT3 plays crucial roles in mitochondrial homeostasis, metabolic modulation, gene transcription, stress response, and genomic stability.[38] For example, SIRT3 promotes NHEJ-dependent DNA damage repair via the deacetylation of H3K56ac.[36] In addition, SIRT3 has been reported to interact with nuclear envelope proteins and heterochromatin-associated proteins.[35] Based on the literature, we hypothesize that SIRT3 also plays an important role in nuclear functions. This hypothesis is further supported by our experimental results (Figure 3C), which suggest that SIRT3 may be involved in nuclear-related activities through the regulation of substrates that undergo lactylation modification. Moreover, Kac proteins regulated by SIRT1 were specifically enriched in the positive regulation of the DNA metabolic process (adjusted $p = 9.89 \times 10^{-11}$), microtubule cytoskeleton organization involved in mitosis (adjusted $p = 4.53 \times 10^{-6}$), and positive regulation of protein localization to the nucleus (adjusted $p = 7.38 \times 10^{-6}$). In contrast, SIRT3-targeted Kac sites were observed to be involved in small molecule catabolic process (adjusted $p = 1.13 \times 10^{-3}$), fatty acid beta-oxidation (adjusted $p = 3.34 \times 10^{-4}$), and carboxylic acid catabolic process (adjusted $p = 4.89 \times 10^{-4}$). Taken together, these results suggested that SIRT1 and SIRT3 may modulate distinct biological processes by differentially modulating the levels of Kla and Kac in specific protein substrates.

Our quantitative proteomics data highlighted an obvious difference between lactylome and acetylome in the absence of SIRT1 or SIRT3, implying a sequence preference for controlling the position of the modification site. Therefore, we compared the amino acid sequences surrounding Kla sites or Kac sites against the human proteome background. Flanking sequence analysis of Kla regulated by SIRT1 and SIRT3 shows similarities, as both exhibit a preference for enriching positively charged lysine at multiple positions (−1, −2, −3, −4, −5, −6, +5, +6), but they also demonstrate differences. For instance, at the +1 position of Kla sites regulated by SIRT1, there is a preference for threonine, while at the same position in Kla sites regulated by SIRT3, a preference for glycine and proline is observed (Figure 3D). In contrast to the sequences at position −1 enriched with lysine and arginine in Kla, the sequences at the same position in Kac regulated by SIRT1 or SIRT3 frequently feature neutral glycine (Figure 3D).

Function analysis of sirtuin 1-and sirtuin 3-targeted lysine lactylation sites

Our recent study has revealed the Kla pathway in lactate metabolism associated with metabolic reprogramming.[5,6] Furthermore, SIRT1 and SIRT3 have been demonstrated to play pivotal roles in metabolism regulation in response to dietary changes.[39] Therefore, we focused on Kla sites related to metabolism regulated by SIRT1 and SIRT3 (Figure 4A), which showed enrichment in pathways such as cysteine and methionine metabolism (adjusted p values are 9.90×10^{-9} and 8.33×10^{-4}, respectively), carbon metabolism (adjusted p values are 9.74×10^{-7} and 8.33×10^{-4}, respectively), glycolysis/gluconeogenesis (adjusted p values are 9.74×10^{-7} and 1.43×10^{-2}, respectively), and biosynthesis of amino acids (adjusted p values are 1.45×10^{-6} and 1.72×10^{-3}, respectively) (Figure 4B). Additionally, propanoate metabolism (adjusted $p = 2.36 \times 10^{-2}$) and alanine, aspartate and glutamate metabolism (adjusted $p = 2.69 \times 10^{-2}$) were exclusively enriched in Kla sites targeted by SIRT1, whereas terpenoid backbone biosynthesis (adjusted $p = 1.97 \times 10^{-2}$) and steroid biosynthesis (adjusted $p = 1.74 \times 10^{-2}$) specific to Kla sites targeted by SIRT3 (Figure 4B). Subsequently, we performed a protein-protein interaction (PPI) network analysis for metabolism-related Kla sites to identify key proteins for further investigation (Figure 4C). Using the cytoHubb plugin and maximal clique centrality (MCC) algorithm, we identified the top 10 hub proteins, including glyceraldehyde-3-phosphate dehydrogenase (GAPDH), phosphoglycerate kinase 1 (PGK1), pyruvate kinase 2 (PKM2), alpha-enolase (ENO1), and so on (Figure 4C). Among these, lactylation at K207 of PKM2 (Figure 4D) was significantly upregulated in the absence of SIRT1 and located within the ATP-binding sites (Figure 4E). Moreover, the deletion of SIRT1 and SIRT3 led to lactylation at K193 and K228 on ENO1 (Figures S4A and S4B).

Furthermore, we explored the potential impact of Kla regulated by SIRT1 or SIRT3 on protein functions (Table 1). Some Kla sites were associated with protein binding and activity. For example, the mutation of K18A on SUMO-conjugating enzyme UBC9 (UBE2I) targeted by SIRT1, which is essential for the SUMOylation of forkhead box protein L2 (FOXL2) and histone acetyltransferase KAT5 (KAT5), impairs its binding to

Table 1. Kla sites on key residues involving protein dysfunctions or substrates/cofactors binding

"Erasers"	Name	Site	Function
SIRT1	PKM2	K207	ATP-binding site
	UBE2I	K18	K→A mutation impairs binding to SUMO1 and catalytic activity
	UPF3B	K434	Missing abolishes nonsense-mediated decay (NMD)
	ENO1	K228	Required for repression of c-myc promoter activity
	EIF3E	K409	Sufficient for interaction with MCM7
SIRT3	ENO1	K228	Required for repression of c-myc promoter activity
	DDX5	K523	Involved in the transactivation domain
	MAP2K4	K45	Cleavage site
	NPM1	K250	Required for nucleolar localization
	PES1	K564	Required for 28S ribosomal RNA processing

SUMO1 and catalytic activity.[40] In addition, K434 of regulator of nonsense transcripts 3B (UPF3B) and K409 of eukaryotic translation initiation factor 3 subunit E (EIF3E), whose lactylation levels could be regulated by SIRT1, are involved in regions required for nonsence-mediated decay (NMD) and interaction with DNA replication licensing factor MCM7 (MCM7), respectively.[41,42] The K564 of pescadillo homolog (PES1), targeted by SIRT3, plays a crucial role in 28S ribosomal RNA processing.[43] These results suggest that Kla proteins mediated by SIRT1 or SIRT3 may impact gene transcription and expression through multiple pathways beyond epigenetics. Interestingly, several Kla sites may be involved in the positioning and cofactor binding site of certain proteins. For instance, K207 of PKM2 regulated by SIRT1 and K45 of dual specificity mitogen-activated protein kinase kinase 4 (MAP2K4) regulated by SIRT3 are located at the ATP-binding site and cleavage site, respectively.[44] Kla at these positions may disrupt the binding interaction. Moreover, a few Kla sites are situated within important protein domains or affected protein localization, such as K523 of probable ATP-dependent RNA helicase (DDX5) regulated by SIRT3 which the transactivation activation domain,[45] and K228 of ENO1 regulated by SIRT1 and SIRT3 necessary for repression of c-myc promoter activity.[46] Overall, these Kla sites offer insights into the biological functions of the substrates regulated by SIRT1 and SIRT3.

Alpha-enolase-K228la is regulated by sirtuin 1 and sirtuin 3 in mammalian cells

Based on the proteomics data analysis above, we identified ENO1 as a lactylated protein with two confidential Kla sites (K193la and K228la) (Figures S4A and S4B). As a glycolysis enzyme, ENO1 participates in various cellular processes such as cell signaling, transcriptional regulation, and apoptosis.[47] Given its diverse functions and involvement in multiple disease pathways, we chose it for further validation. Flag-tagged wild type (WT) ENO1 was overexpressed in HEK293T cells, with or without the treatment of sodium lactate, followed by Flag-immunoprecipitation. Western blot analysis confirmed that WT ENO1 was lactylated, with increased Kla levels upon sodium lactate treatment in HEK293T cells (Figure 5A).

Next, to investigate whether the aforementioned sites are the major Kla site of ENO1, we constructed K193R mutant (MUT) and K228R mutant (MUT) of ENO1 and compared the dynamics of Kla levels between WT and MUT ENO1. Compared with WT ENO1, the K228R mutation of ENO1 in HEK293T cells led to a notable decrease in Kla levels, while the K193R mutation did not, indicating that Kla mainly occurs at K228 of ENO1 (Figure 5B). As the Kla levels of ENO1 improved significantly after SIRT1 KO or SIRT3 KO, to further confirm the regulation of ENO1 lactylation by SIRT1 and SIRT3, we investigated the interaction between SIRT1 and SIRT3 with ENO1. HEK293T cells were transiently co-transfected with Flag-SIRT1/SIRT3 or Flag-vector and HA-ENO1, and total protein extracts were co-immunoprecipitated with Flag beads. The results demonstrated interactions between ENO1 and SIRT1 as well as ENO1 and SIRT3 (Figures 5C and 5D). Moreover, overexpression of SIRT1 or SIRT3 in HEK293T cells obviously reduced the lactylation level of ENO1 (Figures 5E and 5F).

To investigate whether SIRT1 and SIRT3 directly regulate the major lactylated lysine residue (K228) of ENO1, we carried out *in vitro* delactylation reactions using synthetic peptides containing K228la of ENO1 (EGLELLK(la)TAIGK) as the substrate (Figures 5G and 5H). Through LC-MS-MS analysis, corresponding unmodified counterparts were detected, and their levels increased with prolonged reaction time. In contrast, the delactylated peptide was not detected in the absence of SIRT1 or SIRT3. Moreover, SIRT1 has a stronger delactylase activity toward ENO1-K228la than SIRT3. Overall, these results collectively demonstrate that ENO1-K228la is a direct lactylation target of SIRT1 and SIRT3.

ENO1 is a glycolytic enzyme that catalyzes the conversion of 2-phosphoglycerate to phosphoenolpyruvate.[48] We immunopurified ENO1 WT and K228R from HepG2 cells, and subsequently assayed their activities using an ENO1 activity assay kit. The results (Figure S5A) indicated that the K228R mutation enhances the enzymatic activity of ENO1. We then performed the ENO1 activity assay of recombinant wildtype and K228la of ENO1. However, the lactylation at K228 of ENO1 had a minor effect on ENO1 enzyme activity compared to the wild type (Figure S5B). Moreover, in order to demonstrate the physiological relevance of ENO1 lactylation in cells, we established stable HEK293T cell lines with ENO1 knockdown and complementation with ENO1 WT and K228R (Figure S5C) and detected cell proliferation activity. The results (Figures S5D and S5F) showed that the knockdown of ENO1 reduced cell proliferation activity, while complementation with ENO1 WT and ENO1 K228R restored the inhibition of cell proliferation. However, there was no significant difference between ENO1 WT and K228R

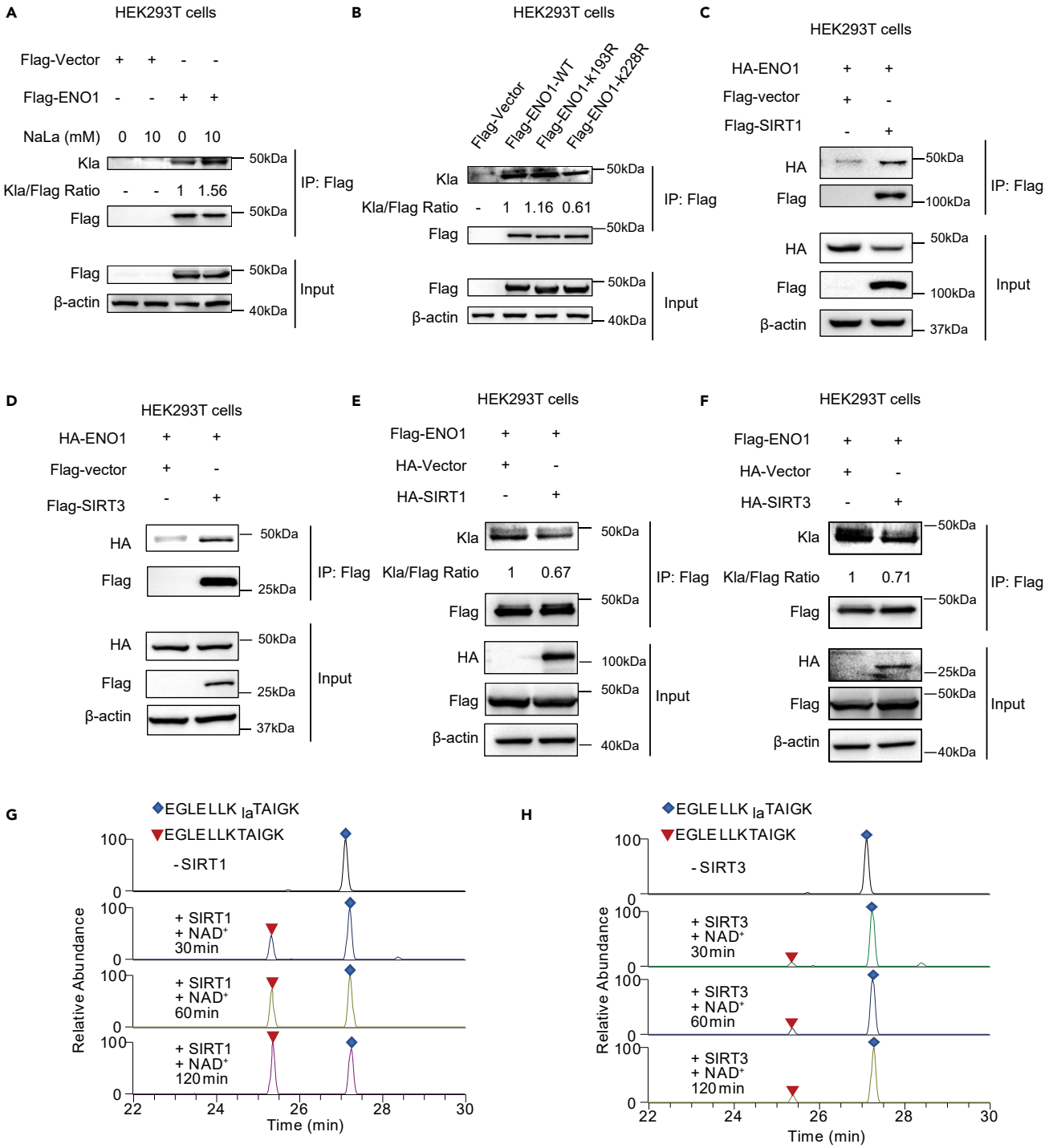

Figure 5. ENO1-K228la is a target of SIRT1 and SIRT3 regulation

(A) Increased Kla levels of ENO1 upon treatment with 10 mM sodium lactate for 24h. HEK293T cells ectopically expressing Flag-vector or Flag-tagged ENO1-WT were stimulated with 10 mM sodium lactate for 24h. Cell lysates underwent immunoprecipitation (IP) with Flag-M2 beads. Inputs and eluates were analyzed by immunoblots.

(B) Lactylation predominantly occurs at K228 of ENO1. HEK293T cells were ectopically expressed with Flag-vector, Flag-tagged ENO1-WT, Flag-tagged ENO1-K193R, and Flag-tagged ENO1-K228R. Cell lysates were subjected to immunoprecipitation (IP) with Flag-M2 beads. Inputs and eluates were analyzed by immunoblots.

Figure 5. *Continued*

(C and D) Interaction of ENO1 with SIRT1 (C) and SIRT3 (D). HEK293T cells were transfected with indicated plasmids, and the association of SIRT1 or SIRT3 with ENO1 was examined by Flag IP and western blot.

(E and F) Reduction of ENO1 Kla by SIRT1 (E) and SIRT3 (F). HEK293T cells were transfected with indicated plasmids, and ENO1 Kla was determined by Flag IP and western blot.

(G and H) SIRT1 and SIRT3 can reduce ENO1 K228la. *In vitro* delactylation reactions were performed with SIRT1 or SIRT3 as enzymes and synthetic Kla peptides containing K228la of ENO1 (EGLELLK(la)TAIGK) as substrates.

in terms of cell proliferation, and treatment with sodium lactate after ENO1 knockdown and complementation with ENO1 WT and ENO1 K228R did not significantly affect cell proliferation, suggesting that ENO1 K228la may not have a significant effect on cell proliferation.

Sirtuin 1 direct regulates pyruvate kinase 2-K207la in mammalian cells

In addition to ENO1, our proteomics data identified PKM2-K207la as a potential target of SIRT1 (Figure 4D). PKM2 is a well-known metabolic enzyme that plays a crucial role in the final step of glycolysis. Apart from its involvement in glycolysis, PKM2 is associated with various cellular processes, including cell signaling, gene expression, and cell proliferation.[49] Importantly, the Kla sites targeted by SIRT1 on PKM2 were identified as K207, located within the ATP-binding site, suggesting its role in potential function regulation (Figure 4E). Therefore, we investigate whether PKM2-K207la is directly regulated by SIRT1. Initially, we found that PKM2 has the capability to undergo lactylation, and the level of lactylation on PKM2 increased upon exposure to sodium lactate in HepG2 cells (Figure 6A).

To confirm that the lactylation of PKM2 primarily occurs at K207, we generated a PKM2 K207R mutant and observed a significant reduction in the overall lactylation of PKM2 compared with the wild-type protein, while its acetylation level only showed slight changes (Figure 6B). This indicates that K207la is the major lactylation site of PKM2, and K207 of PKM2 is primarily lactylated rather than acetylated.

Co-immunoprecipitation and western blotting in HepG2 cells revealed a direct interaction between PKM2 and SIRT1 (Figure 6C). Moreover, overexpression of SIRT1 reduced the levels of Kla and Kac of PKM2 (Figure 6D). However, the effect of SIRT1 on the lactylation level of PKM2 K207R was only marginal (Figure 6E). These results suggest that SIRT1 directly interacts with PKM2 and delactylates it at K207. To further confirm whether PKM2 K207 is a direct delactylation substrate of SIRT1, we specifically induced lactylation of PKM2 at K207 in HepG2 cells and HEK293T cells using genetic code expansion technology. Immunoprecipitation and western blot analysis demonstrated that SIRT1 can interact with PKM2 and reduce the level of K207-specific lactylation (Figures 6F and 6G). However, the impact of SIRT3 on the lactylation level of K207 in PKM2 was relatively minor (Figure 6H). Overall, these results strongly support the notion that K207 of PKM2 is a reversible lactylated lysine and a direct SIRT1 deacetylation substrate, rather than SIRT3.

K207la of pyruvate kinase 2 restricts glycolysis and cell growth by impeding pyruvate kinase 2 function

PKM2 exists in homotetrameric and homodimeric forms.[50] The PKM2 dimer form primarily exhibits low activity, while the tetramer form displays remarkably high activity in the presence of physiological concentrations of phosphoenolpyruvate (PEP). The ratio of tetramer to dimer plays a crucial role in regulating cellular proliferation, survival, and transformation.[50] ATP functions both as a substrate and an allosteric regulator for PKM2, influencing its conformation and activity. The lysine 207 (K207) residue on PKM2 is crucial for ATP binding.[44] Therefore, any modifications to this site, such as lactylation, can disrupt the interaction between PKM2 and ATP, potentially leading to altered enzyme conformation and activity. In addition, several studies have shown that the tetramer-to-dimer transition of PKM2 could be regulated by PTMs, such as acetylation[51] and succinylation.[52]

We further explored whether K207la regulates the conversion of PKM2 from tetramer to dimer. Immunoprecipitation of Flag-PKM2 WT, K207R, and K207la from transfected HEK293T cells, along with disuccinimidyl suberate (DSS) crosslinking experiment, suggested that PKM2 K207la and K207R had significantly lower levels of PKM2 tetramer formation (240KDa) compared with WT (Figure 7A). Furthermore, PKM2 K207la more drastically inhibited tetramer formation than PKM2 K207R. Given that K207 of PKM2 is crucial for ATP binding and K207la of PKM2 remarkably disrupts tetramer formation, thereby affecting pyruvate kinase activity, we performed pyruvate activity assay on immunopurified proteins of Flag-PKM2 WT, K207R, and K207la. Enzyme activity was measured and normalized against protein level (Figure S6A). Obviously, both K207la and K207R mutation significantly decreased PKM2 pyruvate kinase activity compared to PKM2 WT, with PKM2 K207la exhibiting the lowest pyruvate kinase activity (Figure 7B). To further determine the impact of lactylation at PKM2-K207 on glycolysis, endogenous PKM2 was knocked down in HEK293T cells using shPKM2 (Figure S6B), followed by transfection with Flag-tagged PKM2 WT, K207R, and K207la to overexpress these genes, and subsequent Seahorse experiments. The results clearly showed that PKM2 K207la and K207R exhibited decreased extracellular acidification rate (ECAR) levels and inhibition of glycolysis compared to PKM2 WT (Figures 7C and 7D), and protein levels were confirmed by Western blotting (Figure S6C).

The tetrameric and dimeric forms of PKM2 display distinct enzymatic activities. It is reported that PKM2 can translocate into the nucleus in response to various signals, such as EGF receptor activation, and homodimerizes, leading to its conversion into a protein threonine- and tyrosine-protein kinase, which catalyzes the phosphorylation of STAT3 at "Tyr-705".[49,53] Therefore, we detected the effect of K207la of PKM2 on the threonine- and tyrosine-protein kinase activity. The results indicated that K207la of PKM2 inhibited the phosphorylation levels of STAT3 at 'Tyr-705' in HEK293T cells (Figure S6D). In addition, phosphorylation, acetylation, and other PTMs on PKM2 have been reported to mediate its different intracellular localizations, ultimately resulting in specific biological functions.[54] Therefore, we constructed GFP-tagged PKM2 WT, K207R, and K207la plasmids transfected into HEK293T cells and HepG2 cells to investigate whether K207la affects the subcellular localization of PKM2. Through fluorescence microscopy, we observed that PKM2 K207la had significantly different intracellular distributions in HEK293T

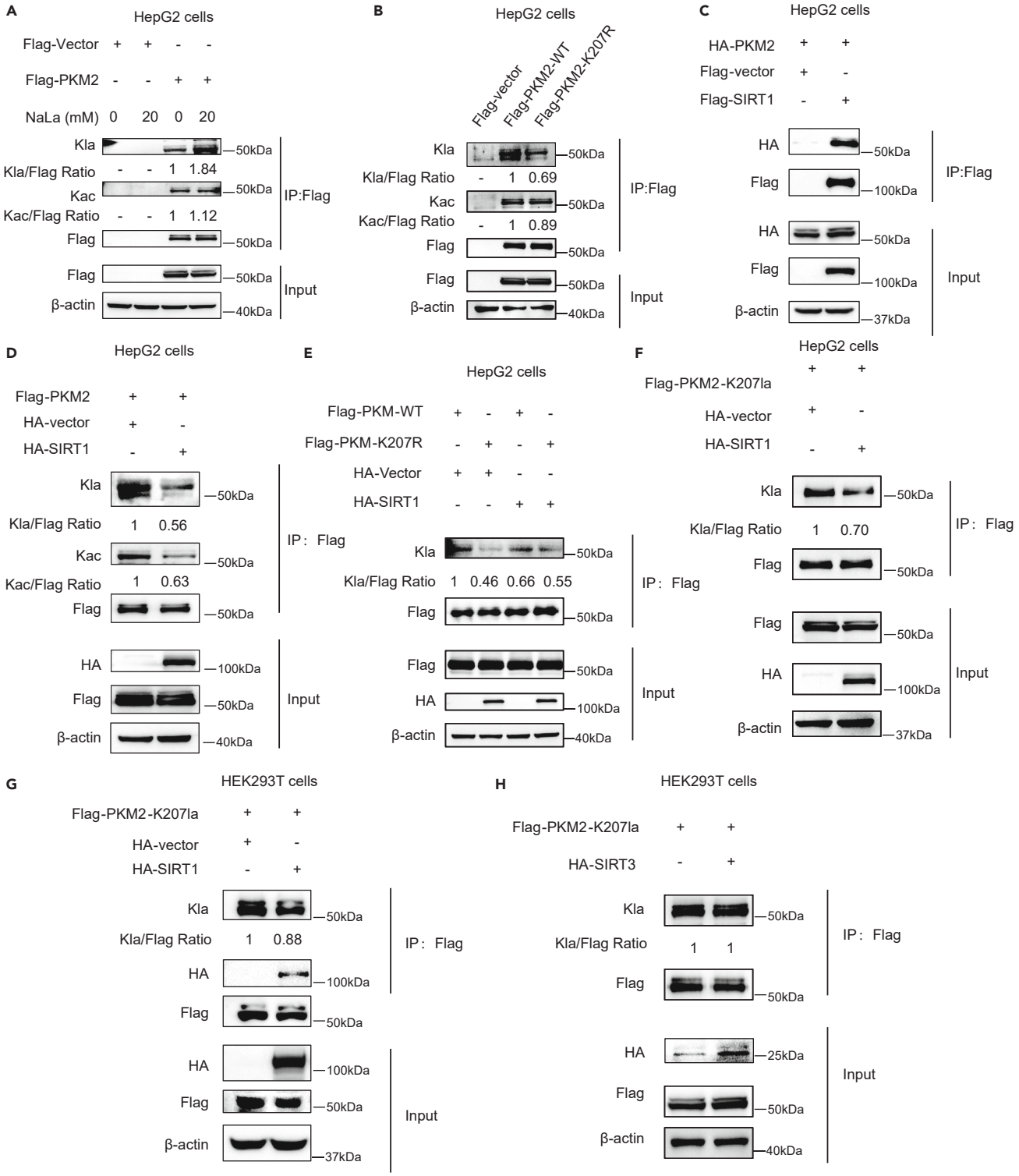

Figure 6. PKM2-K207la is directly regulated by SIRT1

(A) Kla levels of PKM2 increase upon treatment with 10 mM sodium lactate for 24h. HepG2 cells overexpressing Flag-vector or Flag-tagged PKM2-WT were treated with 20 mM sodium lactate for 24h. Cell lysates were subjected to immunoprecipitation (IP) with Flag-M2 beads. Inputs and eluates were analyzed by immunoblots.

(B) Lactylation, not acetylation, primarily occurs at K207 of PKM2. HepG2 cells were ectopically expressed Flag-vector, Flag-tagged PKM2-WT and Flag-tagged PKM2-K207R. Cell lysates were subjected to immunoprecipitation (IP) with Flag-M2 beads. Inputs and eluates were analyzed by immunoblots.

Figure 6. *Continued*

(C) PKM2 interacts with SIRT1. HepG2 cells were transfected with indicated plasmids, and the association between SIRT1 and PKM2 was examined by Flag IP and Western blot.

(D and E) SIRT1 reduces the levels of Kla and Kac of PKM2-WT (D), while SIRT1 has minimal effect on the Kla of PKM2 K207R (E). HepG2 cells were transfected with indicated plasmids, and PKM2 lactylation was determined by Flag IP and Western blot.

(F and G) SIRT1 reduces the PKM2 lactylation at K207. HepG2 cells (F) and HEK293T cells (G) were transfected with K207-specifically lactylated PKM2 using genetic code expansion technology, along with SIRT1. PKM2 lactylation was determined by Flag IP and Western blot.

(H) SIRT3 does not reduce the lactylation of PKM2 at K207. HEK293T cells were transfected with K207-specifically lactylated PKM2 using genetic code expansion technology, along with SIRT3, followed by Flag IP and Western blot analysis.

and HepG2 cells compared to PKM2 WT, while PKM2 K207R had a similar distribution to PKM2 WT (Figures 7E and 7F). This indicates that the lactylation of PKM2-K207 plays a crucial role in modulating PKM2 interactions, leading to distinct intracellular localization patterns.

Considering the significant effects of K207la on PKM2 enzyme activity and subcellular localization, and the reported important roles of PKM2 in cell proliferation,[51,54] we further explored whether lactylation at PKM2-K207 affects the biological behavior of cells. Consistent to previous studies,[55] we observed a decrease in cell proliferation when PKM2 was knocked down (Figure S6E). Furthermore, overexpression of PKM2 K207la in HEK293T cells with endogenous PKM2 knockdown exhibited the lowest proliferation rate, followed by PKM2 K207R and PKM2 WT (Figures 7G and S6F), suggesting a proliferation-inhibiting function of K207 lactylation.

Collectively, these findings illustrate that the lactylation of PKM2 at K207, targeted by SIRT1, determines enzymatic activity by impeding tetramer formation and alters intracellular localization, subsequently inhibiting glycolysis and cell growth.

DISCUSSION

Metabolites not only serve as substrates in metabolic reactions but also function as signaling molecules controlling various cellular processes.[56,57] Lactate, the product of glycolysis in normal physiology and extensively generated during the Warburg effect, is acknowledged as both an energy source and a metabolic byproduct.[58] Its metabolic significance in cancer biology has been appreciated for many decades. Notably, beyond its conventional role as a metabolite, our recent studies have revealed lactate's additional function as a signaling molecule through Kla,[5,6] thus establishing a direct connection between cellular metabolism and the modulation of cell signaling, transcription, and cell growth. Therefore, deciphering the "actylation code" is imperative for understanding its implications on health and diseases.

Exploring the Kla pathway necessitates understanding its regulatory elements, including regulatory enzymes and key substrates. In this study, we performed delactylase activity screening of recombinant sirtuins (SIRT1-7) enzymes using core histones as substrates. Among the seven mammalian sirtuins, SIRT1, SIRT2, and SIRT3 exhibited the most effective delactylase activity *in vitro*. Further overexpression and knockout experiments revealed that SIRT1 and SIRT3, rather than SIRT2, act as robust "erasers" of Kla in mammalian cells, affecting the global substrates including both histones and non-histones.

Moreover, the global proteomic analysis of Kla and Kac in mammalian cells lacking SIRT1 or SIRT3 revealed unique regulatory patterns of SIRT1 and SIRT3 toward these two acylations. Specifically, 1348 unique Kla sites on 724 proteins and 705 unique Kac sites on 477 proteins were upregulated in SIRT1 KO cells compared to WT cells, while 1143 unique Kla sites on 680 proteins and 177 unique Kac sites on 153 proteins showed increased abundance in SIRT3-deficient cells. Notably, the Kla substrates regulated by SIRT1 and SIRT3 were most significantly enriched in the spliceosome pathway, a key component in the processing of pre-mRNA during gene expression. Specifically, SIRT1-targeted Kla proteins were associated with RNA metabolism, suggesting a role for SIRT1 in the control of alternative splicing and the stability of RNA molecules. In contrast, SIRT3 may play a protective role against inflammatory responses and the deleterious effects of alcohol by modulating the lactylation status of certain proteins. Furthermore, SIRT3-target Kac proteins preferred to be enriched in carbon metabolism. These findings underscore the multifaceted roles of SIRT1 and SIRT3 in the regulation of post-translational modifications and their impact on diverse cellular functions. Understanding these regulatory networks can provide valuable insights into the molecular mechanisms underlying various diseases and may open avenues for therapeutic interventions.

Remarkably, we have identified several Kla sites associated with protein dysfunctions or substrates/cofactors binding. Our study revealed that the lactylation level of ENO1 K228, a critical residue involved in repressing c-myc promoter activity, is regulated by SIRT1 and SIRT3. Additionally, the lactylation level at K207 within the ATP-binding site of PKM2 is specifically regulated by SIRT1, affecting PKM2 activity by preventing tetramer formation, thereby impairing glycolysis and inhibiting cell growth.

Collectively, our study identifies SIRT1 and SIRT3 as robust "erasers" of the Kla pathway in mammalian cells and characterizes their specific substrates. Investigating these key regulatory elements of the Kla pathway not only reveals the site-specific functions of substrate lactylation but also expands our understanding of the noncanonical functions of sirtuins. Further functional studies targeting specific Kla sites elucidate the regulatory mechanisms of Kla beyond epigenetics, such as discovering the regulation mechanism of PKM2 K207la, a non-histone Kla site specifically regulated by SIRT1, in cellular glycolysis. These findings provide a perspective on the regulatory mechanisms of Kla and offer insights into lactate metabolism, potentially laying the groundwork for the discovery of strategies for disease treatment.

Limitations of the study

This study confirms that SIRT1 regulates PKM2-K207la. We emphasize the critical role of Kla at PKM2-K207 in influencing protein assembly and enzymatic activity, affecting glycolysis and cell proliferation. However, the biological function studies, performed primarily in HEK293T and HepG2 cell lines, provide valuable insights but are limited in scope. Future research should extend to relevant disease models to fully explore

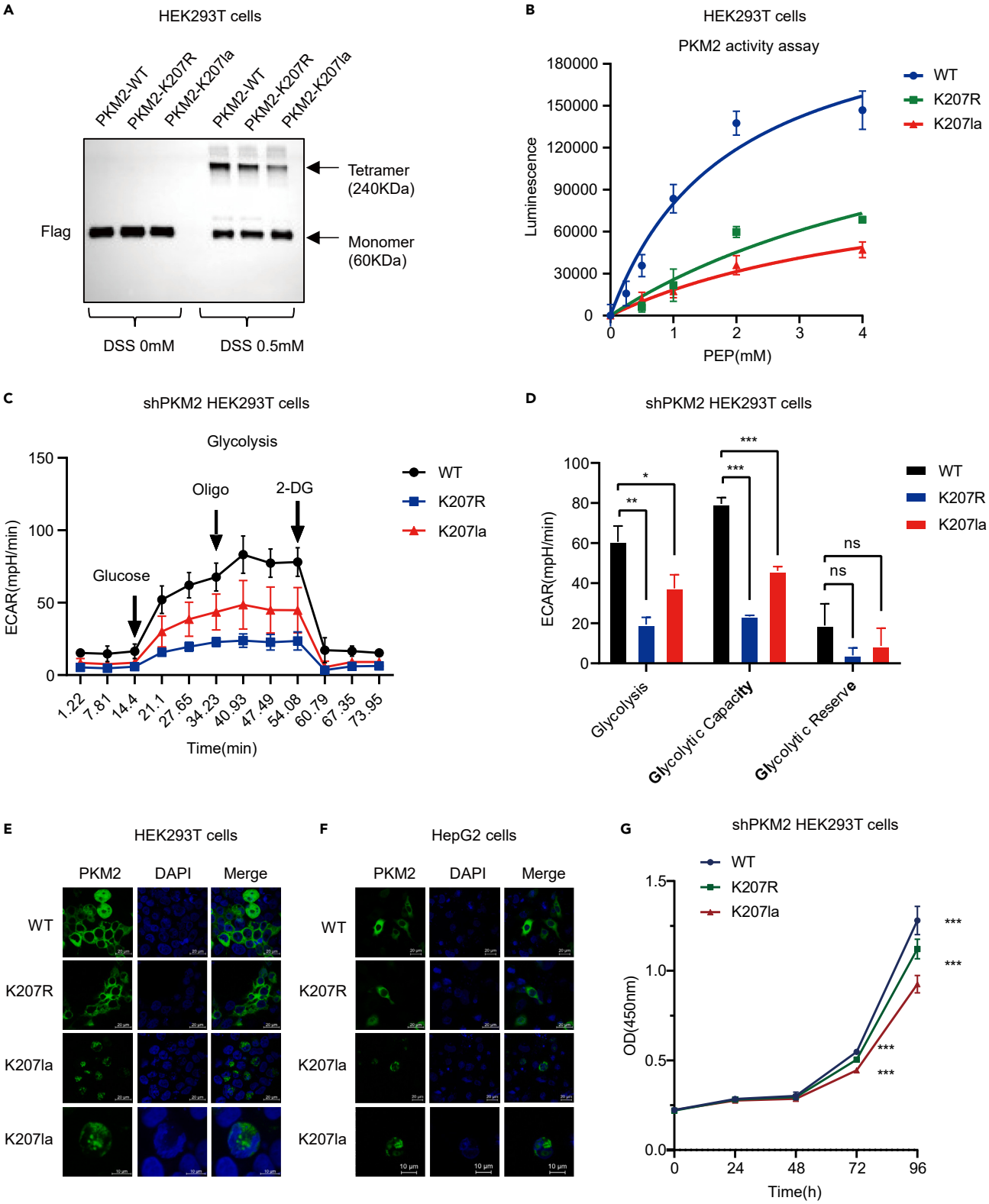
A
HEK293T cells
PKM2-WT
PKM2-K207R
PKM2-K207la
PKM2-WT
PKM2-K207R
PKM2-K207la
Tetramer
(240KDa)
Flag
Monomer
(60KDa)
DSS 0mM
DSS 0.5mM
B
HEK293T cells
PKM2 activity assay
Luminescence
PEP(mM)
WT
K207R
K207la
C
shPKM2 HEK293T cells
Glycolysis
ECAR(mpH/min)
Glucose
Oligo
2-DG
Time(min)
WT
K207R
K207la
D
shPKM2 HEK293T cells
ECAR(mpH/min)
Glycolysis
Glycolytic Capacity
Glycolytic Reserve
ns
WT
K207R
K207la
E
HEK293T cells
PKM2
DAPI
Merge
WT
K207R
K207la
K207la
F
HepG2 cells
PKM2
DAPI
Merge
WT
K207R
K207la
K207la
G
shPKM2 HEK293T cells
WT
K207R
K207la
OD(450nm)
Time(h)

Figure 7. Lactylation status of K207 dictates PKM2 activity, inhibits glycolysis, and affects cell growth

(A) Immunopurified PKM2 WT, K207R, and K207la from HEK293T cells were crosslinked with 0.5mM DSS, and the tetrameric (240 KDa) and monomeric (60 KDa) forms of PKM2 were analyzed by Western blot.

(B) Pyruvate kinase activity assay of immunopurified PKM2 WT, K207R, and K207la from HEK293T cells. Data are represented as mean ± SEM.

(C and D) HEK293T cells with endogenous PKM2 knocked down were transfected with PKM2-WT, K207R, and K207la, and the glycolysis activity was analyzed by the Seahorse analyzer (n = 5 technical repeats, values are expressed as mean ± SEM). p values are calculated by a two-tailed Student's t test. *: $p < 0.05$, **: $p < 0.01$, ***: $p < 0.001$.

(E and F) Representative confocal projections of GFP-tagged PKM2 WT, K207R, and K207la in HEK293T cells (E) and HepG2 cells (F), scale bar = 20 μm or 10 μm.

(G) Cell proliferation analysis of PKM2 knockdown HEK293T cells expressing PKM2-WT, K207R, and K207la by Cell Counting Kit-8 (CCK-8) assay (n = 10 technical repeats, values are expressed as mean ± SEM). p values are calculated by a two-tailed Student's t test. *: $p < 0.05$, **: $p < 0.01$, ***: $p < 0.001$.

Kla's biological significance. Such studies will offer a comprehensive understanding of Kla's role in disease pathogenesis and could lead to therapeutic strategies targeting metabolic dysregulation and epigenetic alterations.

RESOURCE AVAILABILITY

Lead contact

Further information and requests for resources and reagents should be directed to and will be fulfilled by the Lead Contact, Prof. He Huang (hhuang@simm.ac.cn).

Materials availability

This study did not generate new unique reagents.

Data and code availability

- The mass spectrometry proteomics data have been deposited to the ProteomeXchange Consortium via the PRIDE partner repository with the dataset identifier PXD050147.
- Accession numbers are listed in the key resources table. All data reported in this article will be shared by the lead contact upon request.
- This article does not report original code.
- Any additional information required to reanalyze the data reported in this article is available from the lead contact upon request.

ACKNOWLEDGMENTS

This research is supported by the National Natural Science Foundation of China (22277125 and 92253306 to H.H.), Natural Science Foundation of Shanghai (23ZR1474600 to H.H.), and the Shanghai Municipal Science and Technology Major Project (to H.H.).

AUTHOR CONTRIBUTIONS

H.H. conceived, designed, and supervised the study. R.D. and Y.G. performed most of the biological experiments. C.Y. and X.R. prepared the proteomics samples and performed the mass spectrometry analysis. G.L., R.D., H.H., J.R., and M.Z. were involved in the analysis of the proteomics data. S.Q. and X.G. were responsible for constructing the corresponding cell lines and plasmids. X.S. prepared the chemical materials required for the research. H.W., Y.Z., and J.L. contributed to the Seahorse experiments to assess cellular metabolism. R.D. wrote the article and H.H. revised the article.

DECLARATION OF INTERESTS

The authors declare no competing interests.

STAR★METHODS

Detailed methods are provided in the online version of this paper and include the following:

- KEY RESOURCES TABLE
- EXPERIMENTAL MODEL AND STUDY PARTICIPANT DETAILS
  - Cell lines
- METHOD DETAILS
  - Enzymes and histone preparation
  - In vitro Kac and Kla assay
  - Western blot
  - Preparation of cell lysate
  - Trypsin digestion of cell lysate
  - Immunoaffinity enrichment
  - HPLC-MS/MS analysis and database search
  - Bioinformatics analyses
  - Immunoprecipitation
  - SIRT1 and SIRT3 delactylase activity assay
  - Site-specific incorporation of Kla into proteins in mammalian cells and *E.*Coli
  - The expression and purification of PKM2
  - PKM2 crosslinking
  - Fluorescence
  - Pyruvate kinase assay

- Seahorse analysis
- Cell proliferation assay
- QUANTIFICATION AND STATISTICAL ANALYSIS

SUPPLEMENTAL INFORMATION

Supplemental information can be found online at https://doi.org/10.1016/j.isci.2024.110911.

Received: April 1, 2024
Revised: July 16, 2024
Accepted: September 6, 2024
Published: September 10, 2024

REFERENCES

1. Walsh, C.T., Garneau-Tsodikova, S., and Gatto, G.J., Jr. (2005). Protein posttranslational modifications: the chemistry of proteome diversifications. Angew. Chem. Int. Ed. Engl. *44*, 7342–7372. https://doi.org/10.1002/anie.200501023.
2. Dancy, B.M., and Cole, P.A. (2015). Protein lysine acetylation by p300/CBP. Chem. Rev. *115*, 2419–2452. https://doi.org/10.1021/cr500452k.
3. Luo, M. (2018). Chemical and Biochemical Perspectives of Protein Lysine Methylation. Chem. Rev. *118*, 6656–6705. https://doi.org/10.1021/acs.chemrev.8b00008.
4. Cheng, Q., Shi, X.L., Li, Q.L., Wang, L., and Wang, Z. (2024). Current Advances on Nanomaterials Interfering with Lactate Metabolism for Tumor Therapy. Adv. Sci. *11*, e2305662. https://doi.org/10.1002/advs.202305662.
5. Zhang, D., Tang, Z., Huang, H., Zhou, G., Cui, C., Weng, Y., Liu, W., Kim, S., Lee, S., Perez-Neut, M., et al. (2019). Metabolic regulation of gene expression by histone lactylation. Nature *574*, 575–580. https://doi.org/10.1038/s41586-019-1678-1.
6. Yang, Z., Yan, C., Ma, J., Peng, P., Ren, X., Cai, S., Shen, X., Wu, Y., Zhang, S., Wang, X., et al. (2023). Lactylome analysis suggests lactylation-dependent mechanisms of metabolic adaptation in hepatocellular carcinoma. Nat. Metab. *5*, 61–79. https://doi.org/10.1038/s42255-022-00710-w.
7. Wan, N., Wang, N., Yu, S., Zhang, H., Tang, S., Wang, D., Lu, W., Li, H., Delafield, D.G., Kong, Y., et al. (2022). Cyclic immonium ion of lactyllysine reveals widespread lactylation in the human proteome. Nat. Methods *19*, 854–864. https://doi.org/10.1038/s41592-022-01523-1.
8. Jin, J., Bai, L., Wang, D., Ding, W., Cao, Z., Yan, P., Li, Y., Xi, L., Wang, Y., Zheng, X., et al. (2023). SIRT3-dependent delactylation of cyclin E2 prevents hepatocellular carcinoma growth. EMBO Rep. *24*, e56052. https://doi.org/10.15252/embr.202256052.
9. Pan, R.Y., He, L., Zhang, J., Liu, X., Liao, Y., Gao, J., Liao, Y., Yan, Y., Li, Q., Zhou, X., et al. (2022). Positive feedback regulation of microglial glucose metabolism by histone H4 lysine 12 lactylation in Alzheimer's disease. Cell Metab. *34*, 634–648.e6. https://doi.org/10.1016/j.cmet.2022.02.013.
10. Chen, Y., Wu, J., Zhai, L., Zhang, T., Yin, H., Gao, H., Zhao, F., Wang, Z., Yang, X., Jin, M., et al. (2024). Metabolic regulation of homologous recombination repair by MRE11 lactylation. Cell *187*, 294–311.e21. https://doi.org/10.1016/j.cell.2023.11.022.
11. Moreno-Yruela, C., Zhang, D., Wei, W., Bæk, M., Liu, W., Gao, J., Danková, D., Nielsen, A.L., Bolding, J.E., Yang, L., et al. (2022). Class I histone deacetylases (HDAC1-3) are histone lysine delactylases. Sci. Adv. *8*, eabi6696. https://doi.org/10.1126/sciadv.abi6696.
12. Zu, H., Li, C., Dai, C., Pan, Y., Ding, C., Sun, H., Zhang, X., Yao, X., Zang, J., and Mo, X. (2022). SIRT2 functions as a histone delactylase and inhibits the proliferation and migration of neuroblastoma cells. Cell Discov. *8*, 54. https://doi.org/10.1038/s41421-022-00398-y.
13. Jennings, E.Q., Ray, J.D., Zerio, C.J., Trujillo, M.N., McDonald, D.M., Chapman, E., Spiegel, D.A., and Galligan, J.J. (2021). Sirtuin 2 Regulates Protein LactoylLys Modifications. Chembiochem *22*, 2102–2106. https://doi.org/10.1002/cbic.202000883.
14. Fan, Z., Liu, Z., Zhang, N., Wei, W., Cheng, K., Sun, H., and Hao, Q. (2023). Identification of SIRT3 as an eraser of H4K16la. iScience *26*, 107757. https://doi.org/10.1016/j.isci.2023.107757.
15. Chang, H.C., and Guarente, L. (2014). SIRT1 and other sirtuins in metabolism. Trends Endocrinol. Metab. *25*, 138–145. https://doi.org/10.1016/j.tem.2013.12.001.
16. Kosciuk, T., Wang, M., Hong, J.Y., and Lin, H. (2019). Updates on the epigenetic roles of sirtuins. Curr. Opin. Chem. Biol. *51*, 18–29. https://doi.org/10.1016/j.cbpa.2019.01.023.
17. Wu, Q.J., Zhang, T.N., Chen, H.H., Yu, X.F., Lv, J.L., Liu, Y.Y., Liu, Y.S., Zheng, G., Zhao, J.Q., Wei, Y.F., et al. (2022). The sirtuin family in health and disease. Signal Transduct. Target. Ther. *7*, 402. https://doi.org/10.1038/s41392-022-01257-8.
18. Pande, S., and Raisuddin, S. (2023). Molecular and cellular regulatory roles of sirtuin protein. Crit. Rev. Food Sci. Nutr. *63*, 9895–9913. https://doi.org/10.1080/10408398.2022.2070722.
19. Langley, E., Pearson, M., Faretta, M., Bauer, U.M., Frye, R.A., Minucci, S., Pelicci, P.G., and Kouzarides, T. (2002). Human SIR2 deacetylates p53 and antagonizes PML/p53-induced cellular senescence. EMBO J. *21*, 2383–2396. https://doi.org/10.1093/emboj/21.10.2383.
20. Giralt, A., and Villarroya, F. (2012). SIRT3, a pivotal actor in mitochondrial functions: metabolism, cell death and aging. Biochem. J. *444*, 1–10. https://doi.org/10.1042/BJ20120030.
21. Zhang, Q., Siyuan, Z., Xing, C., and Ruxiu, L. (2024). SIRT3 regulates mitochondrial function: A promising star target for cardiovascular disease therapy. Biomed. Pharmacother. *170*, 116004. https://doi.org/10.1016/j.biopha.2023.116004.
22. Shen, Y., Wu, Q., Shi, J., and Zhou, S. (2020). Regulation of SIRT3 on mitochondrial functions and oxidative stress in Parkinson's disease. Biomed. Pharmacother. *132*, 110928. https://doi.org/10.1016/j.biopha.2020.110928.
23. Shen, S., Shen, M., Kuang, L., Yang, K., Wu, S., Liu, X., Wang, Y., and Wang, Y. (2024). SIRT1/SREBPs-mediated regulation of lipid metabolism. Pharmacol. Res. *199*, 107037. https://doi.org/10.1016/j.phrs.2023.107037.
24. Wang, T., Cao, Y., Zheng, Q., Tu, J., Zhou, W., He, J., Zhong, J., Chen, Y., Wang, J., Cai, R., et al. (2019). SENP1-Sirt3 Signaling Controls Mitochondrial Protein Acetylation and Metabolism. Mol. Cell *75*, 823–834.e5. https://doi.org/10.1016/j.molcel.2019.06.008.
25. Alves-Fernandes, D.K., and Jasiulionis, M.G. (2019). The Role of SIRT1 on DNA Damage Response and Epigenetic Alterations in Cancer. Int. J. Mol. Sci. *20*, 3153. https://doi.org/10.3390/ijms20133153.
26. Chen, C., Zhou, M., Ge, Y., and Wang, X. (2020). SIRT1 and aging related signaling pathways. Mech. Ageing Dev. *187*, 111215. https://doi.org/10.1016/j.mad.2020.111215.
27. Silaghi, C.N., Farcas, M., and Crăciun, A.M. (2021). Sirtuin 3 (SIRT3) Pathways in Age-Related Cardiovascular and Neurodegenerative Diseases. Biomedicines *9*, 1574. https://doi.org/10.3390/biomedicines9111574.
28. Shan, P., Fan, G., Sun, L., Liu, J., Wang, W., Hu, C., Zhang, X., Zhai, Q., Song, X., Cao, L., et al. (2017). SIRT1 Functions as a Negative Regulator of Eukaryotic Poly(A)RNA Transport. Curr. Biol. *27*, 2271–2284.e5. https://doi.org/10.1016/j.cub.2017.06.040.
29. Ansari, A., Rahman, M.S., Saha, S.K., Saikot, F.K., Deep, A., and Kim, K.H. (2017). Function of the SIRT3 mitochondrial deacetylase in cellular physiology, cancer, and neurodegenerative disease. Aging Cell *16*, 4–16. https://doi.org/10.1111/acel.12538.
30. Palomer, X., Román-Azcona, M.S., Pizarro-Delgado, J., Planavila, A., Villarroya, F., Valenzuela-Alcaraz, B., Crispi, F., Sepúlveda-Martínez, Á., Miguel-Escalada, I., Ferrer, J., et al. (2020). SIRT3-mediated inhibition of FOS through histone H3 deacetylation prevents cardiac fibrosis and inflammation. Signal Transduct. Target. Ther. *5*, 14. https://doi.org/10.1038/s41392-020-0114-1.
31. Nasrin, N., Kaushik, V.K., Fortier, E., Wall, D., Pearson, K.J., de Cabo, R., and Bordone, L. (2009). JNK1 phosphorylates SIRT1 and promotes its enzymatic activity. PLoS One *4*, e8414. https://doi.org/10.1371/journal.pone.0008414.

32. Ding, X., Zhu, C., Wang, W., Li, M., Ma, C., and Gao, B. (2024). SIRT1 is a regulator of autophagy: Implications for the progression and treatment of myocardial ischemia-reperfusion. Pharmacol. Res. *199*, 106957. https://doi.org/10.1016/j.phrs.2023.106957.
33. Celestini, V., Tezil, T., Russo, L., Fasano, C., Sanese, P., Forte, G., Peserico, A., Lepore Signorile, M., Longo, G., De Rasmo, D., et al. (2018). Uncoupling FoxO3A mitochondrial and nuclear functions in cancer cells undergoing metabolic stress and chemotherapy. Cell Death Dis. *9*, 231. https://doi.org/10.1038/s41419-018-0336-0.
34. Ning, Y., Dou, X., Wang, Z., Shi, K., Wang, Z., Ding, C., Sang, X., Zhong, X., Shao, M., Han, X., and Cao, G. (2024). SIRT3: A potential therapeutic target for liver fibrosis. Pharmacol. Ther. *257*, 108639. https://doi.org/10.1016/j.pharmthera.2024.108639.
35. Diao, Z., Ji, Q., Wu, Z., Zhang, W., Cai, Y., Wang, Z., Hu, J., Liu, Z., Wang, Q., Bi, S., et al. (2021). SIRT3 consolidates heterochromatin and counteracts senescence. Nucleic Acids Res. *49*, 4203–4219. https://doi.org/10.1093/nar/gkab161.
36. Sengupta, A., and Haldar, D. (2018). Human sirtuin 3 (SIRT3) deacetylates histone H3 lysine 56 to promote nonhomologous end joining repair. DNA Repair *61*, 1–16. https://doi.org/10.1016/j.dnarep.2017.11.003.
37. Scher, M.B., Vaquero, A., and Reinberg, D. (2007). SirT3 is a nuclear NAD+-dependent histone deacetylase that translocates to the mitochondria upon cellular stress. Genes Dev. *21*, 920–928. https://doi.org/10.1101/gad.1527307.
38. Lombard, D.B., and Zwaans, B.M.M. (2014). SIRT3: as simple as it seems? Gerontology *60*, 56–64. https://doi.org/10.1159/000354382.
39. Michan, S., and Sinclair, D. (2007). Sirtuins in mammals: insights into their biological function. Biochem. J. *404*, 1–13. https://doi.org/10.1042/BJ20070140.
40. Tatham, M.H., Kim, S., Yu, B., Jaffray, E., Song, J., Zheng, J., Rodriguez, M.S., Hay, R.T., and Chen, Y. (2003). Role of an N-terminal site of Ubc9 in SUMO-1, -2, and -3 binding and conjugation. Biochemistry *42*, 9959–9969. https://doi.org/10.1021/bi0345283.
41. Gehring, N.H., Neu-Yilik, G., Schell, T., Hentze, M.W., and Kulozik, A.E. (2003). Y14 and hUpf3b form an NMD-activating complex. Mol. Cell *11*, 939–949. https://doi.org/10.1016/s1097-2765(03)00142-4.
42. Buchsbaum, S., Morris, C., Bochard, V., and Jalinot, P. (2007). Human INT6 interacts with MCM7 and regulates its stability during S phase of the cell cycle. Oncogene *26*, 5132–5144. https://doi.org/10.1038/sj.onc.1210314.
43. Grimm, T., Hölzel, M., Rohrmoser, M., Harasim, T., Malamoussi, A., Gruber-Eber, A., Kremmer, E., and Eick, D. (2006). Dominant-negative Pes1 mutants inhibit ribosomal RNA processing and cell proliferation via incorporation into the PeBoW-complex. Nucleic Acids Res. *34*, 3030–3043. https://doi.org/10.1093/nar/gkl378.
44. Morgan, H.P., O'Reilly, F.J., Wear, M.A., O'Neill, J.R., Fothergill-Gilmore, L.A., Hupp, T., and Walkinshaw, M.D. (2013). M2 pyruvate kinase provides a mechanism for nutrient sensing and regulation of cell proliferation. Proc. Natl. Acad. Sci. USA *110*, 5881–5886. https://doi.org/10.1073/pnas.1217157110.
45. Rossow, K.L., and Janknecht, R. (2003). Synergism between p68 RNA helicase and the transcriptional coactivators CBP and p300. Oncogene *22*, 151–156. https://doi.org/10.1038/sj.onc.1206067.
46. Ghosh, A.K., Steele, R., and Ray, R.B. (1999). Functional domains of c-myc promoter binding protein 1 involved in transcriptional repression and cell growth regulation. Mol. Cell Biol. *19*, 2880–2886. https://doi.org/10.1128/MCB.19.4.2880.
47. Qiao, G., Wu, A., Chen, X., Tian, Y., and Lin, X. (2021). Enolase 1, a Moonlighting Protein, as a Potential Target for Cancer Treatment. Int. J. Biol. Sci. *17*, 3981–3992. https://doi.org/10.7150/ijbs.63556.
48. Sugahara, T., Nakajima, H., Shirahata, S., and Murakami, H. (1992). Purification and characterization of immunoglobulin production stimulating factor-II beta derived from Namalwa cells. Cytotechnology *10*, 137–146. https://doi.org/10.1007/BF00570890.
49. Gao, X., Wang, H., Yang, J.J., Liu, X., and Liu, Z.R. (2012). Pyruvate kinase M2 regulates gene transcription by acting as a protein kinase. Mol. Cell *45*, 598–609. https://doi.org/10.1016/j.molcel.2012.01.001.
50. Lv, L., Xu, Y.P., Zhao, D., Li, F.L., Wang, W., Sasaki, N., Jiang, Y., Zhou, X., Li, T.T., Guan, K.L., et al. (2013). Mitogenic and oncogenic stimulation of K433 acetylation promotes PKM2 protein kinase activity and nuclear localization. Mol. Cell *52*, 340–352. https://doi.org/10.1016/j.molcel.2013.09.004.
51. Park, S.H., Ozden, O., Liu, G., Song, H.Y., Zhu, Y., Yan, Y., Zou, X., Kang, H.J., Jiang, H., Principe, D.R., et al. (2016). SIRT2-Mediated Deacetylation and Tetramerization of Pyruvate Kinase Directs Glycolysis and Tumor Growth. Cancer Res. *76*, 3802–3812. https://doi.org/10.1158/0008-5472.CAN-15-2498.
52. Wang, F., Wang, K., Xu, W., Zhao, S., Ye, D., Wang, Y., Xu, Y., Zhou, L., Chu, Y., Zhang, C., et al. (2017). SIRT5 Desuccinylates and Activates Pyruvate Kinase M2 to Block Macrophage IL-1beta Production and to Prevent DSS-Induced Colitis in Mice. Cell Rep. *19*, 2331–2344. https://doi.org/10.1016/j.celrep.2017.05.065.
53. Yang, W., Xia, Y., Ji, H., Zheng, Y., Liang, J., Huang, W., Gao, X., Aldape, K., and Lu, Z. (2011). Nuclear PKM2 regulates beta-catenin transactivation upon EGFR activation. Nature *480*, 118–122. https://doi.org/10.1038/nature10598.
54. Zhang, Z., Deng, X., Liu, Y., Liu, Y., Sun, L., and Chen, F. (2019). PKM2, function and expression and regulation. Cell Biosci. *9*, 52. https://doi.org/10.1186/s13578-019-0317-8.
55. Stone, O.A., El-Brolosy, M., Wilhelm, K., Liu, X., Romão, A.M., Grillo, E., Lai, J.K.H., Günther, S., Jeratsch, S., Kuenne, C., et al. (2018). Loss of pyruvate kinase M2 limits growth and triggers innate immune signaling in endothelial cells. Nat. Commun. *9*, 4077. https://doi.org/10.1038/s41467-018-06406-8.
56. Huang, H., Lin, S., Garcia, B.A., and Zhao, Y. (2015). Quantitative proteomic analysis of histone modifications. Chem. Rev. *115*, 2376–2418. https://doi.org/10.1021/cr500491u.
57. Huang, H., Sabari, B.R., Garcia, B.A., Allis, C.D., and Zhao, Y. (2014). SnapShot: histone modifications. Cell *159*, 458–458.e1. https://doi.org/10.1016/j.cell.2014.09.037.
58. Vaupel, P., Schmidberger, H., and Mayer, A. (2019). The Warburg effect: essential part of metabolic reprogramming and central contributor to cancer progression. Int. J. Radiat. Biol. *95*, 912–919. https://doi.org/10.1080/09553002.2019.1589653.
59. Tolia, N.H., and Joshua-Tor, L. (2006). Strategies for protein coexpression in Escherichia coli. Nat. Methods *3*, 55–64. https://doi.org/10.1038/nmeth0106-55.
60. Shechter, D., Dormann, H.L., Allis, C.D., and Hake, S.B. (2007). Extraction, purification and analysis of histones. Nat. Protoc. *2*, 1445–1457. https://doi.org/10.1038/nprot.2007.202.
61. Du, R., Liu, G., and Huang, H. (2022). Deep 2-Hydroxyisobutyrylome in mouse liver expands the roles of lysine 2-hydroxyisobutyrylation pathway. Bioorg. Med. Chem. *57*, 116634. https://doi.org/10.1016/j.bmc.2022.116634.
62. Colaert, N., Helsens, K., Martens, L., Vandekerckhove, J., and Gevaert, K. (2009). Improved visualization of protein consensus sequences by iceLogo. Nat. Methods *6*, 786–787. https://doi.org/10.1038/nmeth1109-786.
63. Mi, H., Poudel, S., Muruganujan, A., Casagrande, J.T., and Thomas, P.D. (2016). PANTHER version 10: expanded protein families and functions, and analysis tools. Nucleic Acids Res. *44*, D336–D342. https://doi.org/10.1093/nar/gkv1194.
64. Falcon, S., and Gentleman, R. (2007). Using GOstats to test gene lists for GO term association. Bioinformatics *23*, 257–258. https://doi.org/10.1093/bioinformatics/btl567.
65. Giurgiu, M., Reinhard, J., Brauner, B., Dunger-Kaltenbach, I., Fobo, G., Frishman, G., Montrone, C., and Ruepp, A. (2019). CORUM: the comprehensive resource of mammalian protein complexes-2019. Nucleic Acids Res. *47*, D559–D563. https://doi.org/10.1093/nar/gky973.
66. Huttlin, E.L., Bruckner, R.J., Paulo, J.A., Cannon, J.R., Ting, L., Baltier, K., Colby, G., Gebreab, F., Gygi, M.P., Parzen, H., et al. (2017). Architecture of the human interactome defines protein communities and disease networks. Nature *545*, 505–509. https://doi.org/10.1038/nature22366.
67. Schweppe, D.K., Huttlin, E.L., Harper, J.W., and Gygi, S.P. (2018). BioPlex Display: An Interactive Suite for Large-Scale AP-MS Protein-Protein Interaction Data. J. Proteome Res. *17*, 722–726. https://doi.org/10.1021/acs.jproteome.7b00572.

STAR★METHODS

KEY RESOURCES TABLE

REAGENT or RESOURCE	SOURCE	IDENTIFIER
Antibodies		
anti-H3K14la	PTM Biolabs	PTM-1414RM; RRID:AB_3076697
anti-H3K18la	PTM Biolabs	PTM-1406RM; RRID:AB_2909438
anti-H4K5la	PTM Biolabs	PTM-1407
anti-H4K8la	PTM Biolabs	PTM-1415
anti-H4K12la	PTM Biolabs	PTM-1411RM; RRID:AB_2941896
anti-H3K14ac	PTM Biolabs	PTM-113; RRID:AB_2722570
anti-H3K18ac	PTM Biolabs	PTM-158
anti-H4K5ac	PTM Biolabs	PTM-119
anti-H4K8ac	PTM Biolabs	PTM-164
anti-H4K12ac	PTM Biolabs	PTM-165
pan anti-Kla	PTM Biolabs	PTM-1401RM; RRID:AB_2942013
pan anti-Kac	PTM Biolabs	PTM-101; RRID:AB_2940830
anti-Histone H3	Huabio	M1306-4; RRID:AB_3073062
anti-Flag	Sigma-Aldrich	F3165; RRID:AB_259529
anti-β-actin	Proteintech	66009-1-Ig; RRID:AB_2687938
anti-SIRT1	PTM Biolabs	PTM-5021
anti-SIRT3	Proteintech	10099-1-AP; RRID:AB_2239240
anti-GST	Proteintech	10000-0-AP; RRID:AB_11042316
anti-His	Proteintech	66005-1-Ig; RRID:AB_11232599
anti-STAT3	abcam	ab119352; RRID:AB_10901752
anti-p-STAT3-Y705	abcam	ab76315; RRID:AB_1658549
anti-ENO1	PTM Biolabs	PTM-7348
anti-PKM2	PTM Biolabs	PTM-5087
HRP-labeled goat anti-rabbit IgG	Beyotime	A0208
HRP-labeled goat anti-mouse IgG	Beyotime	A0216
Bacterial and virus strains		
Trans1-T1 Phage Resistant Chemically Competent Cell	TransGen Biotech	CD501-02
BL21(DE3) pLysS Chemically Competent Cell	TransGen Biotech	CD701-02
Chemicals, peptides, and recombinant proteins		
DSS	Sangon Biotech	C100015-0100
Sodium lactate	Sigma	71718
Hieff TransTM Liposomal Transfection Reagent	YEASEN	Y40802ES03
ANTI-FLAG ® M2 Affinity Gel	Sigma	A2220
DAPI	Beyotime	C1002
Precision Plus Protein Dual Color Standards	BIO-RAD	1610374
ColorMixed Protein Marker	ABclonal	RM02949
Recombinant human GST-Sirtuin 1 (193-741)	This paper	N/A
Recombinant human His-Sirtuin 2 (50-356)	This paper	N/A
Recombinant human GST-Sirtuin 3 (102-399)	This paper	N/A
Recombinant human GST-Sirtuin 4 (25-314)	This paper	N/A

(*Continued on next page*)

Continued

REAGENT or RESOURCE	SOURCE	IDENTIFIER
Recombinant human His-Sirtuin 5	This paper	N/A
Recombinant human His-Sirtuin 6	This paper	N/A
Recombinant human His-Sirtuin 7	This paper	N/A
Lactyllysine	This paper	N/A
EGLELLK(la)TAIGK	This paper	N/A
Deposited data		
Identified Kla peptides (see also Table S1)	ProteomeXchange	PXD050147
Identified Kac peptides (see also Table S2)	ProteomeXchange	PXD050147
Critical commercial assays		
ADP-Glo™ kinase assay kit	Promega Corporation	V6930
ENO1 assay kit	Abcam	ab117994
Cell Counting Kit-8	Beyotime	C0040
Experimental models: cell lines		
HEK293T	ATCC	CRL-3216
HepG2	ATCC	HB-8065
Oligonucleotides		
sgRNA for hSIRT1 5′ GTTGACTGTGAAGCTGTACG 3′	This paper	N/A
sgRNA for hSIRT3 5′ GTACGATCTCCCGTACCCCG 3′	This paper	N/A
siRNA for hPKM2 acatcaagattatcagcaa	This paper	N/A
siRNA for hENO1 agtccttgatgaaggactt	This paper	N/A
Recombinant DNA		
pFLAG-CMV-SIRT1	This paper	N/A
pFLAG-CMV-SIRT2	This paper	N/A
pFLAG-CMV-SIRT3	This paper	N/A
pGEX-4T-1-Sirtuin 1 (193-741)	This paper	N/A
pET-28a (+)-Sirtuin 2 (50-356)	This paper	N/A
pGEX-4T-1-Sirtuin 3 (102-399)	This paper	N/A
pGEX-4T-1-Sirtuin 4 (25-314)	This paper	N/A
pET-28a (+)-His-Sirtuin 5	This paper	N/A
pET-28a (+)-His-Sirtuin 6	This paper	N/A
pET-28a (+)-His-Sirtuin 7	This paper	N/A
pFLAG-CMV-ENO1-WT	This paper	N/A
pFLAG-CMV-PKM2-WT	This paper	N/A
pFLAG-CMV-ENO1-K193R	This paper	N/A
pFLAG-CMV-ENO1-K228R	This paper	N/A
pFLAG-CMV-PKM2-K207R	This paper	N/A
pFLAG-CMV-PKM2-K207*	This paper	N/A
pBAD-ENO1-WT	This paper	N/A
pBAD-ENO1-K228*	This paper	N/A

(*Continued on next page*)

Continued

REAGENT or RESOURCE	SOURCE	IDENTIFIER
Software and algorithms		
GraphPad Prism (v 9.3.1)	GraphPad Software	https://www.graphpad.com/scientific-software/prism/
ImageJ	ImageJ software	https://imagej.nih.gov/ij/index.html
R (v4.2.3)	R software	https://www.r-project.org/
MaxQuant (version 1.6.15.0)	MaxQuant software	https://www.maxquant.org/
Cytoscape (v3.3.0)	Cytoscape software	https://cytoscape.org/
ZEN 3.0 (blue edition)	ZEN Microscopy Software	https://www.zeiss.com/microscopy/en/products/software/zeiss-zen.html
PyMOL (v3.0)	PyMOL software	https://pymol.org/
iceLogo (v1.3.8)	iceLogo software	https://compomics.github.io/projects/iceLogo

EXPERIMENTAL MODEL AND STUDY PARTICIPANT DETAILS

Cell lines

Human embryonic kidney (HEK) 293T and human hepatocellular carcinomas (HepG2) cells were cultured in DMEM medium supplemented with 10% FBS, 1% P/S (penicillin and streptomycin), and 5% CO2. Transient overexpression was achieved through transfection using Hieff TransTM Liposomal Transfection Reagent, following the manufacturer's instructions.

HepG2 cells were transfected with either an empty vector lentiCRISPRv2 or a SIRT1 knockout vector lentiCRISPRv2-sgRNA (SIRT1) to establish two stable cell lines. Similarly, depletion of SIRT3 was accomplished using analogous methods. The knockout efficiency, as well as the levels of Kla and Kac, were evaluated by western blot analysis using whole-cell lysate extractions.

HEK293T cells were seeded in a six-well plate at 50% density one day before transfection. Three plasmids, including the backbone plasmid shRNA vector GIPZ targeting PKM2, packaging plasmid psPAX2, and envelope plasmid pMD2.G (mass ratio = 4:3:3), were co-transfected into HEK293T cells with 80–90% density. The medium was changed at 12 h, replenished at 36 h, and harvested at 48 and 72 h after transfection. Puromycin was used to eliminate non-infected cells, and only resistant clones were selected and cultured. When almost all cells in the control group died, the screening process was completed, indicating that effective KD clones were obtained.

METHOD DETAILS

Enzymes and histone preparation

SIRT1-7 enzymes were individually purified according to a previously reported method.[59] Firstly, the targeted genes (SIRT1-7) were cloned into the desired vector (pGEX-4T-1 or pET-28a (+)). Secondly, each clone was transformed into BL21 (DE3) for screening of a suitable expression clone induced by IPTG. Finally, appropriate expression clones were used for large-scale expression. Briefly, a starter culture was initiated by inoculating glycerol stock into 200 mL of LB supplemented with appropriate antibiotics (depending on the plasmids present) and incubated at 37°C until OD600 reached 0.6–1. Subsequently, 200 μL of 0.5 M IPTG (final concentration ranged from 0.1 to 1 mM) was added, and the culture was incubated for 2 h. The resulting pellets were harvested by centrifugation at 5000×*g* for 15 min and lysed by sonication until the cloudy suspension became translucent. After centrifuging at 16000×*g* for 30 min, the soluble target proteins were purified by affinity chromatography based on the tags present.

Histone proteins were extracted using the previously published method.[60] Briefly, HEK293T cells were suspended in cold extraction buffer (10 mM HEPES pH 7.0, 10 mM KCl, 1.5 mM $MgCl_2$, 0.34 M sucrose, 0.5% NP-40) at 4°C for 30 min. After centrifugation, the pellets were re-suspended in cold washing buffer (10 mM HEPES pH 7.0, 10 mM KCl, 1.5 mM $MgCl_2$, 0.34 M sucrose) and centrifuged. Then, the pellets were extracted with 0.2 M H_2SO_4 at 4°C overnight. After centrifugation at 16000×*g* for 10 min at 4°C, the histone proteins were precipitated by slowly adding 20% (v/v) TCA to the supernatants. The resulting histone pellets were washed twice with cold, dried at 4°C, dissolved in double distilled water, and subjected to protein concentration determination with Bradford assay.

In vitro Kac and Kla assay

For each *in vitro* reaction, 1 μg of Sirtuin (SIRT1-7) and 4 μg of histone proteins were added to the reaction buffer (20 mM Tris-Cl, pH 8.0, 1 mM DTT, and 1 mM NAD^+). The mixtures were incubated at 37°C for 0.5 h, and the levels of Kac and Kla were detected by western blot.

Western blot

Proteins (2–4 μg of histone or 20 μg of whole cell lysate) were separated in SDS-PAGE and then transferred to a polyvinylidene difluoride membrane. The membrane was blocked with 3% BSA in TBST (20 mM Tris, pH 7.6; 150 mM NaCl, 0.1% Tween 20) for 1 h at room temperature and then incubated overnight at 4°C with a primary antibody. Following incubation, the membrane was washed 3 times with TBST and incubated

with horseradish peroxidase-conjugated secondary antibody solutions for 1 h at room temperature. Subsequently, the membrane was washed again in TBST before detecting the signal using an enhanced chemiluminescence system.

Preparation of cell lysate

The harvested cells were rinsed twice with cold PBS and subsequently sonicated for 2 min on ice using ultrasonication in lysis buffer (8 M urea, 2 mM EDTA, 3 μM TSA, 50 mM NAM, 5 mM DTT, and 1% Protease Inhibitor Cocktail III). After centrifugation at 16 000×*g* at 4°C for 10 min, the concentration of the supernatant was determined using the Bradford assay.

Trypsin digestion of cell lysate

Proteins extracted from WT, SIRT1KO, and SIRT3KO HepG2 cells were subjected to in-solution tryptic digestion. Briefly, the proteins were reduced by 10 mM DTT for 1.5 h at 37°C, followed by alkylation with 20 mM iodoacetamide (IAA) at room temperature in the dark for 30 min. Excess IAA was then blocked by 20 mM cysteine. After that, the protein sample was diluted by adding 100 mM NH_4HCO_3 to reduce the urea concentration to 2 M. Then trypsin was added into the solution for the first digestion (trypsin: protein = 1:50, m/m; pH 8.0, overnight) and second digestion (trypsin: protein = 1:100, m/m; pH 8.0, 4 h).

Immunoaffinity enrichment

Kla and Kac peptides were enriched using the pan anti-Kla antibody and pan anti-Kac antibody, respectively, as previous described.[61] Briefly, the peptides were dissolved in NETN buffer (100 mM NaCl, 50 mM Tris-HCl, 1 mM EDTA, 0.5% NP-40, pH 8.0) and incubated with pan anti-Kla beads or pan anti-Kac beads at 4°C overnight. Then, the beads were washed three times with NETN buffer and twice with ddH_2O. The enriched peptides were eluted with 0.1% (v/v) TFA and dried in SpeedVac.

HPLC-MS/MS analysis and database search

An EASY-nLC 1200 UHPLC system (ThermoFisher Scientific) coupled with a Q Exactive HF-X mass spectrometer (ThermoFisher Scientific) was employed for peptide analysis. The peptide samples were dissolved in 2.5 μL of buffer A (0.1% formic acid in water, v/v) and trapped on a homemade capillary C18 column (25 cm length×75 μm inner diameter) packed with 1.9 μm ReproSil-Pur C18-AQ particles (Dr. Maisch, Germany). Peptides were separated using a gradient of 6%–90% buffer B (0.1% formic acid in 80% ACN) over 180- and 120-min gradient, respectively.

Data acquisition was carried out in positive ion data-dependent mode, with an MS scan range of 350–1200 m/z acquired in the Orbitrap at a resolution of 60,000. The 20 most intense ions were subjected to collision-induced dissociation fragmentation with a normalized collision energy at 28%. MS/MS scans were acquired at a resolution of 15,000. The unassigned ions or those with a charge of +1 and >+5 were rejected. The time for dynamic exclusion was set to 30.0 s.

For the label-free quantification method, raw data were uploaded into MaxQuant (version 1.6.15.0) and searched against the UniProt reviewed human proteome sequence database (20,368 entries). The parameters to analyze raw data were that maximum missed cleavages digested by trypsin/P were 2, and maximum FDR for peptides and proteins of 1%. Cysteine carbamidomethylation (+57.0215 Da) was established as a fixed modification, and methionine oxidation (+15.9949 Da) and N-terminal acetylation (+42.0106 Da) were designated as variable modifications. Parameter setting of Kla and Kac samples included lysine lactyl (+72.0211 Da) and lysine acetyl (+42.0106 Da), respectively, as variable modifications. The remaining of the parameters were in accordance with the proteome search. FDR thresholds for modification site sites were specified at 1%, and the LFQ algorithm were performed. The quantified protein expression levels were used to normalize all of the Kla and Kac site ratios.

Bioinformatics analyses

Sequence motif preference was generated using iceLogo (v1.3.8) with the human proteome as the background.[62] Gene ontology analysis was performed using Bonferroni correction for multiple testing in PANTHER (v12.0).[63] Identified Kla and Kac sites were mapped with reported binding and mutation sites extracted from the UniProt database (http://www.uniprot.org). KEGG pathway enrichment analysis was carried out using the GOstats package along with a hypergeometric test in R.[64] Protein complexes were enriched based on CORUM mammalian protein complex database[65] using the hypergeometric test. The protein complexes of interest were further described using BioPlex 2.0[66,67] based on the known PPI network and finally visualized in Cytoscape (v3.3.0).

Immunoprecipitation

For immunoprecipitation experiments, relevant plasmids were transfected into either HEK293T or HepG2 cells using Hieff TransTM Liposomal Transfection Reagent for 48 h, with 10 mM or 20 mM sodium lactate treatment for the last 24 h. Cells were then harvested and lysed in cell lysis buffer (20 mM Tris-HCl pH 7.4, 150 mM sodium chloride and 1% Triton X-100) containing a protease inhibitor cocktail for 40 min at 4°C. Soluble supernatant fractions were obtained by centrifugation at 16,000 g for 10 min and used for immunoprecipitation with Flag beads. After binding, the beads were washed three times with immunoprecipitation lysis buffer to remove the non-specifically bound proteins.

SIRT1 and SIRT3 delactylase activity assay

For each *in vitro* reaction, 1 μg of Sirtuin (SIRT1 or SIRT3) and 0.5 μM Kla peptide (EGLELLK(la)TAIGK) were added to the reaction buffer (20 mM Tris-Cl, pH 8.0, 1 mM DTT, and 1 mM NAD^+). The mixtures were incubated at 37°C for 0.5 h, 1h and 2h, respectively. Then, the reaction was stopped by adding 50 μL of 200 mM HCl and 320 mM acetic acid in methanol. The samples were dried and analyzed by HPLC-MS/MS. Product quantification was based on their peak areas.

Site-specific incorporation of Kla into proteins in mammalian cells and *E.Coli*

A pCMV-3′ Flag vector with a human PKM2 gene incorporating an amber stop codon at a specific lysine coding position (K207) and pNEU_hMb_KlaRS were co-transfected into HEK293T cells or HepG2 cells using Hieff TransTM Liposomal Transfection Reagent, following the manufacturer's instructions. The cells were cultured in the presence of 2 mM lactyllysine for 48 h. A pBAD vector with a human ENO1 gene incorporating an amber stop codon at a specific lysine coding position (K228) and pEVOL-Mm_KlaRS-137976 were co-transformed into DH10B for screening of a suitable expression clone induced by L-Arabinose. Finally, appropriate expression clones were used for large-scale expression.

The expression and purification of PKM2

The relevant plasmids were transfected into HEK293T cells using Hieff TransTM Liposomal Transfection Reagent, following the manufacturer's instructions. Proteins were immunoprecipitated with Flag beads and washed two times with immunoprecipitation lysis buffer and PBS, respectively, to remove non-specifically bound proteins. Competitively elution of proteins from Flag beads was achieved with peptides containing 10 ng/μL 1× Flag peptide (dissolved in PBS) for 4 h. Finally, purified proteins were mixed with 50% glycerol in equal volumes and stored in portions frozen at −80°C.

PKM2 crosslinking

The equal amount of PKM2 WT, K207R, and K207la proteins purified from cells were crosslinked with 0.5 mM DSS at room temperature for 30 min. The reaction was halted with 25 mM Tris pH 7.5 at room temperature for 15 min. Samples were then separated followed by western blotting with anti-Flag antibody.

Fluorescence

Plasmids encoding WT, K207R, and K207la PKM2 genes tagged with GFP were transfected into HEK293T or HepG2 cells cultured on slides. The cells were fixed with paraformaldehyde, permeabilized with 0.5% Triton X-100 at room temperature. After incubation with DAPI, the slides were imaged using a Zeiss confocal microscope, and images were analyzed with Zeiss LSM software.

Pyruvate kinase assay

The equal amount of WT, K207R, and K207la PKM2 purified from HEK293T cells were added into the reaction buffer (500 μM ADP, 40 mM Tris pH 8.0, 20 mM $MgCl_2$, 100 mM KCl and 0.1 g/mL BSA) with different concentration of PEP ranging from 0 to 4 mM, respectively, at 32°C for 5 min. Pyruvate kinase activity was determined using the ADP-Glo kinase assay kit according to the manufacturer's instructions.

Seahorse analysis

Assays were performed using the Seahorse XFp analyzer (Seahorse Bioscience, Agilent) following the manufacturer's instructions. Briefly, 2×10^4 HEK293T cells were seeded into each well of Seahorse XF96 Cell Culture Microplates in growth medium 24 h prior to the assay. The extracellular acidification rate (ECAR) was measured using an XFp analyzer in XF base medium (pH 7.4) containing 1 mM glutamine following sequential additions of glucose (10 mM), oligomycin (1 μM), and 2-DG (100 mM). Data were analyzed using the Seahorse XF Glycolysis Stress Test Report Generator package.

Cell proliferation assay

Cell proliferation ability was assessed using the Cell Counting Kit-8. 2×10^3 cells transfected with Flag-tagged PKM2 WT/K207R/K207la plasmids for 18 h or PKM2 WT/PKM2 knockdown stable cell lines were seeded into a 96-well plate per well with ten or five duplications, followed by incubation for 1 h at 37°C. Absorbance was detected at 450 nm daily for 5 consecutive days.

QUANTIFICATION AND STATISTICAL ANALYSIS

All data were processed and analyzed by the unpaired two-tailed Student's t test or the hypergeometric test in R. Statistical significance is indicated with asterisks as follows: ns, no significance; *, $p < 0.05$; **, $p < 0.01$; ***, $p < 0.001$; ****, $p < 0.0001$.